

Existence and stability of viscoelastic shock profiles

BLAKE BARKER *MARTA LEWICKA †KEVIN ZUMBRUN ‡

June 12, 2010

Abstract

We investigate existence and stability of viscoelastic shock profiles for a class of planar models including the incompressible shear case studied by Antman and Malek–Madani. We establish that the resulting equations fall into the class of symmetrizable hyperbolic–parabolic systems, hence spectral stability implies linearized and nonlinear stability with sharp rates of decay. The new contributions are treatment of the compressible case, formulation of a rigorous nonlinear stability theory, including verification of stability of small-amplitude Lax shocks, and the systematic incorporation in our investigations of numerical Evans function computations determining stability of large-amplitude and or nonclassical type shock profiles.

1 Introduction

In this paper, generalizing work of Antman and Malek–Madani [AM] in the incompressible shear flow case, we carry out the numerical and analytical study of the existence and stability of planar viscoelastic traveling waves in a 3d solid, for a simple prototypical elastic energy density, both for the general compressible and the incompressible shear flow case. We establish that the resulting equations fall into the class of symmetrizable hyperbolic–parabolic systems studied in [MaZ2, MaZ3, MaZ4, RZ, Z4], hence spectral stability implies linearized and nonlinear stability with sharp rates of decay. This important point was previously left undecided, due to a lack of the necessary abstract stability framework.

The new contributions beyond what was done in [AM] are: treatment of the compressible case, consideration of large-amplitude waves (somewhat artificial given our simple choice of energy density; however, the methods used clearly generalize to more physically correct models), formulation of a rigorous nonlinear stability theory including verification

*Indiana University, Bloomington, IN 47405; bhbarker@indiana.edu: Research of B.B. was partially supported under NSF grant no. DMS-0801745.

†Department of Mathematics, University of Minnesota 206 Church S.E., Minneapolis, MN 55455; lewicka@math.umn.edu: Research of M.L. was partially supported under NSF grants no. DMS-0707275 and DMS-0846996.

‡Indiana University, Bloomington, IN 47405; kzumbrun@indiana.edu: Research of K.Z. was partially supported under NSF grants no. DMS-0300487 and DMS-0801745.

of stability of small-amplitude Lax waves, and the systematic incorporation in our investigations of numerical Evans function computations determining stability of large-amplitude and or nonclassical type shock profiles. For related analysis in various different settings, see [BHRZ, HLZ, HLYZ, CHNZ, BHZ, BLZ].

In preparation for future generalizations, we also discuss the case of phase-transitional viscoelasticity. It would be interesting to carry out similar analysis for more general classes of elastic energy density, as well as for the phase-transitional case which involves, at the technical level higher order dispersive terms relating to surface energy, and at the physical level, presumably, interesting new behaviors.

Acknowledgment. Thanks to Stuart Antman and Constantine Dafermos for several helpful conversations, and to Stuart Antman for making available the working notes [A].

2 The equations of viscoelasticity

The equations of isothermal viscoelasticity are given by the balance of linear momentum:

$$(2.1) \quad \xi_{tt} - \nabla_X \cdot \left(DW(\nabla\xi) + \mathcal{Z}(\nabla\xi, \nabla\xi_t) \right) = 0.$$

Here, $\xi : \Omega \times \mathbb{R}_+ \rightarrow \mathbb{R}^3$ denotes the deformation of a reference configuration $\Omega \subset \mathbb{R}^3$ which models a viscoelastic body with constant temperature and density. A typical point in Ω is denoted by X , so that the deformation gradient is given as:

$$F = \nabla\xi \in \mathbb{R}^{3 \times 3},$$

with the key constraint of:

$$\det F > 0.$$

In (2.1) the operator $\nabla_X \cdot$ stands for the divergence of an appropriate field. We use the convention that the divergence of a matrix field is taken row-wise. In what follows, we shall also use the matrix norm $|F| = (\text{tr}(F^T F))^{1/2}$, which is induced by the inner product: $F_1 : F_2 = \text{tr}(F_1^T F_2)$.

The mapping $DW : \mathbb{R}^{3 \times 3} \rightarrow \mathbb{R}^{3 \times 3}$ is the Piola-Kirchhoff stress tensor which, in agreement with the second law of thermodynamics, is expressed as the derivative of an elastic energy density $W : \mathbb{R}^{3 \times 3} \rightarrow \overline{\mathbb{R}}_+$. The viscous stress tensor is given by the mapping $\mathcal{Z} : \mathbb{R}^{3 \times 3} \times \mathbb{R}^{3 \times 3} \rightarrow \mathbb{R}^{3 \times 3}$, depending on the deformation gradient F and the velocity gradient $Q = F_t = \nabla\xi_t = \nabla v$, where $v = \xi_t$.

The first order version of the inviscid part of (2.1):

$$(2.2) \quad \xi_{tt} - \nabla_X \cdot \left(DW(\nabla\xi) \right) = 0$$

is:

$$(2.3) \quad (F, v)_t + \sum_{i=1}^3 \partial_{X_i} (\tilde{G}_i(F, v)) = 0.$$

Above, $(F, v) : \Omega \longrightarrow \mathbb{R}^{12}$ represents conserved quantities, while $\tilde{G}_i : \mathbb{R}^{12} \longrightarrow \mathbb{R}^{12}$ given by:

$$-\tilde{G}_i(F, v) = v^1 e_i \oplus v^2 e_i \oplus v^3 e_i \oplus \left[\frac{\partial}{\partial F_{ki}} W(F) \right]_{k=1}^3, \quad i = 1..3$$

are the fluxes, and e_i denotes the i -th coordinate vector of \mathbb{R}^3 .

2.1 The elastic energy density W

The principle of material frame invariance imposes the following condition on W , with respect to the group $SO(3)$ of proper rotations in \mathbb{R}^3 :

$$(2.4) \quad W(RF) = W(F) \quad \forall F \in \mathbb{R}^{3 \times 3} \quad \forall R \in SO(3).$$

Also, the material consistency requires that:

$$(2.5) \quad W(F) \rightarrow +\infty \quad \text{as } \det F \rightarrow 0.$$

In what follows, we shall restrict our attention to the class of isotropic materials, for whom the energy W satisfies additionally:

$$(2.6) \quad W(FR) = W(F) \quad \forall F \in \mathbb{R}^{3 \times 3} \quad \forall R \in SO(3).$$

Recall [Ba] that hyperbolicity of (2.2) is equivalent to rank-one convexity of W .

A particular example of W satisfying (2.4) and (2.6) is:

$$(2.7) \quad W_0(F) = \frac{1}{4} |F^T F - \text{Id}|^2 = \frac{1}{4} (|F^T F|^2 - 2|F|^2 + 3)$$

and by a direct calculation, we obtain:

$$DW_0(F) = F(F^T F - \text{Id}).$$

Note that W_0 in (2.7) is not quasiconvex (or polyconvex) as it is not globally rank-one convex. This follows by checking the Legendre-Hadamard condition. Indeed, for any $A \in \mathbb{R}^{3 \times 3}$ one has: $\partial_{AA}^2 W_0(F) = (FA^T F + FF^T A + AF^T F - A) : A$. Taking $A = \text{Id}$ and $F \in \text{skew}$ we obtain $\partial_{AA}^2 W_0(F) = |F|^2 - 3$ which is negative for $|F| < \sqrt{3}$.

On the other hand we see that $\partial_{AA}^2 W_0(R) = 2|\text{sym}(AR^T)|^2$ for $R \in SO(3)$. If $\text{rank } A = 1$ then $\text{rank}(AR^T) = 1$ so $\text{sym}(AR^T) \neq 0$. Therefore $\partial_{AA}^2 W_0(R) \geq c|A|^2$ for every $R \in SO(3)$ and every rank-one matrix A , with a uniform $c > 0$. This implies that W_0 is rank-one convex in a neighborhood of $SO(3)$.

Notice also that W_0 has quadratic growth close to $SO(3)$. Indeed, write $F = R + E$, where for F close to $SO(3)$ we have: $R = \mathbb{P}_{SO(3)} F$ and $|E| = \text{dist}(F, SO(3))$. Since E is orthogonal to the tangent space to $SO(3)$ at R , we see that $R^T E$ must be symmetric. Therefore: $W_0(F) = \frac{1}{4} |R^T E + E^T R + E^T E|^2 = \frac{1}{4} |2R^T E + E^T E|^2 = |E|^2 + \mathcal{O}(|E|^3)$.

For other examples of W satisfying (2.4) and (2.6), see (3.7) and Appendix A.1.

2.2 The viscous stress tensor \mathcal{Z}

The viscous stress tensor $\mathcal{Z} : \mathbb{R}^{3 \times 3} \times \mathbb{R}^{3 \times 3} \longrightarrow \mathbb{R}^{3 \times 3}$ should be compatible with the following principles of continuum mechanics: balance of angular momentum, frame invariance, and the Clausius-Duhem inequality. That is, for every $F, Q \in \mathbb{R}^{3 \times 3}$ with $\det F \neq 0$, we require that:

- (i) skew $(F^{-1}\mathcal{Z}(F, Q)) = 0$, i.e. $\mathcal{Z} = FS$ with S symmetric.
- (2.8) (ii) $\mathcal{Z}(RF, R_tF + RQ) = R\mathcal{Z}(F, Q)$ for every path of rotations $R : \mathbb{R}_+ \longrightarrow SO(3)$,
i.e. in view of (i): $S(RF, RKQ) = S(R, Q) \forall R \in SO(3) \forall K \in \text{skew}$.
- (iii) $\mathcal{Z}(F, Q) : Q \geq 0$, i.e. in view of (i): $S : \text{sym}(F^T Q) \geq 0$.

Examples of \mathcal{Z} satisfying the above are:

$$(2.9) \quad \begin{aligned} \mathcal{Z}_1(F, Q) &= 2F \text{sym}(F^T Q), \\ \mathcal{Z}_2(F, Q) &= 2(\det F) \text{sym}(QF^{-1})F^{-1,T}. \end{aligned}$$

We note that in the case of \mathcal{Z}_2 , the related Cauchy stress tensor $T_2 = 2(\det F)^{-1} \mathcal{Z}_2 F^T = 2 \text{sym}(QF^{-1})$ is the Lagrangian version of the stress tensor $2 \text{sym} \nabla v$ written in Eulerian coordinates. For incompressible fluids $2 \text{div}(\text{sym} \nabla v) = \Delta v$, giving the usual parabolic viscous regularization of the fluid dynamics evolutionary system. For more general viscous stress tensors, see Appendix A.2.

2.3 An extension: the surface energy

A phenomenological modification that is sometimes used is to replace (2.1) with

$$(2.10) \quad \xi_{tt} - \nabla_X \cdot \left(DW(\nabla \xi) + \mathcal{Z}(\nabla \xi, \nabla \xi_t) - \mathcal{E}(\nabla^2 \xi) \right) = 0,$$

where the surface energy \mathcal{E} is given by:

$$\mathcal{E}(\nabla^2 \xi) = \nabla_X \cdot D\Psi(\nabla^2 \xi) = \left[\sum_{i=1}^3 \frac{\partial}{\partial X_i} \left(\frac{\partial}{\partial (\partial_{ij} \zeta^k)} \Psi(\nabla^2 \xi) \right) \right]_{j,k:1\dots 3}$$

for some convex density $\Psi : \mathbb{R}^{3 \times 3 \times 3} \longrightarrow \mathbb{R}$, compatible with frame indifference (and isotropy). A typical example is $\Psi_0(G) = \frac{1}{2}|G|^2$, so that:

$$(2.11) \quad \mathcal{E}_0(\nabla^2 \xi) = \nabla_X \cdot \nabla^2 \xi = \Delta_X F$$

which is an extension of the 1d case of [Sl].

Writing the variation of the energy $\int \Psi(\nabla^2 \xi)$ in the direction of a test function $\phi \in \mathcal{C}_c^\infty(\Omega, \mathbb{R}^3)$ we obtain:

$$(2.12) \quad \int_{\Omega} D\Psi(\nabla^2 \xi) : \nabla^2 \phi = \int_{\Omega} (\nabla_X \cdot \mathcal{E}(\nabla^2 \xi)) \cdot \phi,$$

which justifies the last divergence term in (2.10).

The addition of surface energy is motivated by the van der Waals/Cahn–Hilliard approach to the stationary equilibrium theory [Sl, Z8, CGS, SZ]. This would be an interesting direction for further investigation.

2.4 Entropy

After integrating (2.1) against ξ_t on Ω , and then integrating by parts, we obtain:

$$\frac{1}{2} \int \partial_t |\xi_t|^2 + \int \left(DW(\nabla\xi) + \mathcal{Z}(\nabla\xi, \nabla\xi_t) \right) : \nabla\xi_t = 0,$$

where we used that:

$$\xi_t^T (DW(\nabla\xi) + \mathcal{Z}(\nabla\xi, \nabla\xi_t)) \vec{n} = 0 \quad \text{on } \partial\Omega,$$

a natural assumption following from either (Dirichlet) clamped boundary conditions $\xi|_{\partial\Omega} = \text{const}$ or else free (Neumann) conditions $(DW(\nabla\xi) + \mathcal{Z}(\nabla\xi, \nabla\xi_t))|_{\partial\Omega} = 0$ corresponding to the absence of stress on the boundary.

Consequently:

$$\partial_t \int \left(\frac{1}{2} \partial_t |\xi_t|^2 + DW(\nabla\xi) \right) = - \int \mathcal{Z}(\nabla\xi, \nabla\xi_t) : \nabla\xi_t \leq 0$$

by the Clausius–Duhem inequality, and we see that the integral $\int \eta$ of the quantity:

$$(2.13) \quad \eta(F, v) = \frac{1}{2} |v|^2 + W(F)$$

along $F = \nabla\xi$ and $v = \xi_t$, is nonincreasing in time. In case of (2.10), using (2.12) with $\phi = \xi_t$ we obtain that $\int \tilde{\eta}$ is nonincreasing, for:

$$\tilde{\eta} = \frac{1}{2} |\xi_t|^2 + W(\nabla\xi) + D\Psi(\nabla^2\xi).$$

Further, notice that $\eta : \mathbb{R}^{12} \rightarrow \mathbb{R}$ defined in (2.13) is an entropy [D] associated to (2.3). Indeed, the scalar fields:

$$q_i(F, v) = -v \cdot \left[\frac{\partial}{\partial F_{ik}} W(F) \right]_{k=1}^3 \quad i = 1..3$$

define the respective entropy fluxes, in the sense that:

$$\nabla q_i(F, v) = \nabla \eta(F, v) D\tilde{G}_i(F, v).$$

3 The planar case

We now restrict our attention to the interesting subclass of planar solutions, which are solutions in full 3d space that depend only on a single coordinate direction. Namely, we assume that the deformation ξ has the form:

$$\xi(X) = X + U(z), \quad X = (x, y, z), \quad U = (u, v, w) \in \mathbb{R}^3,$$

which yields the following structure of the deformation gradient:

$$(3.1) \quad F = \begin{bmatrix} 1 & 0 & u_z \\ 0 & 1 & v_z \\ 0 & 0 & 1 + w_z \end{bmatrix} = \begin{bmatrix} 1 & 0 & a_1 \\ 0 & 1 & a_2 \\ 0 & 0 & a_3 \end{bmatrix}.$$

We shall denote $V = (a, b) = (a_1, a_2, a_3, b_1, b_2, b_3)$, where $a_1 = u_z, a_2 = v_z, a_3 = 1 + w_z$ and $b_1 = u_t, b_2 = v_t, b_3 = w_t$, with the constraint:

$$(3.2) \quad a_3 > 0,$$

corresponding to $\det F > 0$ in the region of physical feasibility of V .

Writing $W(a) = W\left(\begin{bmatrix} 1 & 0 & a_1 \\ 0 & 1 & a_2 \\ 0 & 0 & a_3 \end{bmatrix}\right)$, we see that for all F as in (3.1) there holds:

$$\nabla_X \cdot (DW(F)) = (D_a W(a))_z.$$

That is, the planar equations inherit a vector-valued variational structure echoing the matrix-valued variational structure, and thus (2.2) has the following form:

$$V_t + G(V)_z = 0$$

$$(3.3) \quad G(V) = (-b, -D_a W(a))^T, \quad DG(V) = \begin{bmatrix} 0 & -\text{Id}_3 \\ -M & 0 \end{bmatrix}, \quad M = D_a^2 W(a).$$

It follows that strict hyperbolicity of (3.3) is equivalent to strict convexity of W with M having 3 distinct (positive) eigenvalues. Also, $\eta(V) = \frac{1}{2}|b|^2 + W(a)$ is then a convex entropy:

$$(3.4) \quad \nabla \eta(V) DG(V) = \nabla q(V), \quad q(V) = -b \cdot D_a W(a).$$

3.1 Energy density W_0 and viscosities \mathcal{Z}_i

By a straightforward calculation, we have:

$$(3.5) \quad W_0(a) = \frac{1}{4}(|a|^2 - 1)^2 + \frac{1}{2}(a_1^2 + a_2^2)$$

and:

$$\begin{aligned}
\operatorname{div}(DW_0(F)) &= \left(u_{zz} + (u_z|U_z|^2 + 2u_z w_z)_z, v_{zz} + (v_z|U_z|^2 + 2v_z w_z)_z, \right. \\
(3.6) \quad & \left. 2w_{zz} + (|U_z|^2 + w_z|U_z|^2 + 2w_z^2)_z \right)^T \\
&= \left((|a|^2 a_1)_z, (|a|^2 a_2)_z, (|a|^2 - 1)a_3 \right)_z^T,
\end{aligned}$$

More generally, one may consider densities of the form:

$$(3.7) \quad W(F) = \frac{1}{4}|F^T F - \operatorname{Id}|^2 + c_2(|F|^2 - 3)^2 + c_3(|\det F| - 1)^2.$$

The c_2 term contributes to $DW(F)$ as: $4c_2(|F|^2 - 3)F$ in the planar case; this is $4c_2(2w_z + |U_z|^2)F$, with divergence:

$$\begin{aligned}
4c_2 \left((u_z|U_z|^2 + 2u_z w_z)_z, (v_z|U_z|^2 + 2v_z w_z)_z, (|U_z|^2 + 2w_z + w_z|U_z|^2 + 2w_z^2)_z \right)^T \\
= 4c_2 \left((|a|^2 - 1)a_1)_z, (|a|^2 - 1)a_2)_z, (|a|^2 - 1)a_3)_z \right)^T.
\end{aligned}$$

The c_3 term contributes to $DW(F)$ the term: $2(\det F - 1)\operatorname{cof} F$, for F with $\det F > 0$. In the planar case, divergence of this term reads $2c_3(0, 0, w_{zz})^T = 2c_3(0, 0, (a_3)_z)^T$.

Combining, we obtain the general form:

$$(3.8) \quad \operatorname{div}(DW(F)) = \left(((\mu_1|a|^2 + \mu_2)a_1)_z, ((\mu_1|a|^2 + \mu_2)a_2)_z, ((\mu_1|a|^2 + \mu_2)a_3 + (\mu_3 - 1)a_3)_z \right)^T,$$

with $\mu_1 = 1 + 4c_2$, $\mu_2 = -4c_2$, $\mu_3 = 2c_3$, corresponding to elastic potential

$$W(a) = \frac{1}{4}\mu_1|a|^4 + \frac{1}{2}\mu_2|a|^2 + \frac{1}{2}\mu_3(a_3 - 1)^2 + C,$$

where C is a constant. The above potential is strictly convex at the identity ($a = (0, 0, 1)$) whenever $\mu_1 + \mu_2 > 0$ and $3\mu_1 + \mu_2 + \mu_3 > 0$. It is a simple case of the general form $W(a) = \tilde{\sigma}(|a|^2, a_3)$ described in Appendix A.1. Restricted to the incompressible planar case of Section 3.2.2, (3.8) recovers the class of equations studied in [AM].

Regarding the viscous tensors, we obtain:

$$\begin{aligned}
\operatorname{div}(\mathcal{Z}_1(F, \dot{F})) &= \left(u_{zzt} + (u_z(2w_{zt} + (|U_z|^2)_t))_z, v_{zzt} + (v_z(2w_{zt} + (|U_z|^2)_t))_z, \right. \\
(3.9) \quad & \left. 2w_{zzt} + (|U_z|^2)_{zt} + (w_z(2w_{zt} + (|U_z|^2)_t))_z \right)^T \\
&= \left((b_{1,z} + 2a_1 a \cdot b_z)_z, (b_{2,z} + 2a_2 a \cdot b_z)_z, (2a_3 a \cdot b_z)_z \right)^T,
\end{aligned}$$

$$\begin{aligned}
\operatorname{div}(\mathcal{Z}_2(F, \dot{F})) &= \left(\left(\frac{u_{zt}}{1 + w_z} \right)_z, \left(\frac{v_{zt}}{1 + w_z} \right)_z, \left(\frac{2w_{zt}}{1 + w_z} \right)_z \right)^T \\
(3.10) \quad &= \left(\left(\frac{b_{1,z}}{a_3} \right)_z, \left(\frac{b_{2,z}}{a_3} \right)_z, 2 \left(\frac{b_{3,z}}{a_3} \right)_z \right)^T,
\end{aligned}$$

where $a \cdot b_z = a_1 b_{1,z} + a_2 b_{2,z} + a_3 b_{3,z}$.

Hence, (2.1) with W and \mathcal{Z} as in (2.7) and (2.9), has the hyperbolic-parabolic form:

$$(3.11) \quad V_t + G(V)_z = (B(V)V_z)_z$$

with $G(V)$ as in (3.3) and:

$$M = D_a^2 W_0 = \text{diag}(|a|^2, |a|^2, |a|^2 - 1) + 2a \otimes a$$

in view of (3.5). Further:

$$(3.12) \quad B = \begin{bmatrix} 0 & 0 \\ 0 & B_{0,i} \end{bmatrix}, \quad B_{0,1} = \text{diag}(1, 1, 0) + 2a \otimes a \quad \text{or} \quad B_{0,2} = \frac{1}{a_3} \text{diag}(1, 1, 2)$$

in case of \mathcal{Z}_1 and \mathcal{Z}_2 , respectively. Both tensors $B_{0,i}$ are symmetric and positive definite on the entire physical region $a_3 > 0$.

3.2 The full and the restricted systems in hyperbolic–parabolic form

3.2.1 Compressible viscoelasticity

For the viscous stress tensor \mathcal{Z}_1 , system (3.11) reads:

$$(3.13) \quad \begin{aligned} a_{1,t} - b_{1,z} &= 0, & b_{1,t} - (|a|^2 a_1)_z &= (b_{1,z} + 2a_1 a \cdot b_z)_z \\ a_{2,t} - b_{2,z} &= 0, & b_{2,t} - (|a|^2 a_2)_z &= (b_{2,z} + 2a_2 a \cdot b_z)_z \\ a_{3,t} - b_{3,z} &= 0, & b_{3,t} - (|a|^2 - 1)a_3)_z &= (2a_3 a \cdot b_z)_z. \end{aligned}$$

For the viscous tensor \mathcal{Z}_2 we have:

$$(3.14) \quad \begin{aligned} a_{1,t} - b_{1,z} &= 0, & b_{1,t} - (|a|^2 a_1)_z &= \left(\frac{b_{1,z}}{a_3} \right)_z, \\ a_{2,t} - b_{2,z} &= 0, & b_{2,t} - (|a|^2 a_2)_z &= \left(\frac{b_{2,z}}{a_3} \right)_z, \\ a_{3,t} - b_{3,z} &= 0, & b_{3,t} - (|a|^2 - 1)a_3)_z &= 2 \left(\frac{b_{3,z}}{a_3} \right)_z. \end{aligned}$$

3.2.2 The 2D incompressible shear case

For an incompressible medium and a shear deformation where $w = 0$, the system (3.14) reduces to the following one (naturally, we now denote $a = (a_1, a_2)$ and $|a|^2 = a_1^2 + a_2^2$):

$$(3.15) \quad \begin{aligned} a_{1,t} - b_{1,z} &= 0, & b_{1,t} - (|a|^2 + 1)a_1)_z &= b_{1,zz}, \\ a_{2,t} - b_{2,z} &= 0, & b_{2,t} - (|a|^2 + 1)a_2)_z &= b_{2,zz}, \end{aligned}$$

with an associated pressure of $p = |a|^2$ whose gradient $(0, 0, (|a|^2)_z)^T$ cancels the term $-(|a|^2)_z$ in the b_3 equation of (3.14). Note that the viscous stress tensor in this case reduces

to the Laplacian. Equations (3.15) are a special case of the equations studied in [AM]; they may be also recognized as the model for an elastic string.

For the choice \mathcal{Z}_1 , we obtain:

$$(3.16) \quad \begin{aligned} a_{1,t} - b_{1,z} &= 0, & b_{1,t} - ((|a|^2 + 1)a_1)_z &= (b_{1,z} + 2a_1 a \cdot b_z)_z, \\ a_{2,t} - b_{2,z} &= 0, & b_{2,t} - ((|a|^2 + 1)a_2)_z &= (b_{2,z} + 2a_2 a \cdot b_z)_z. \end{aligned}$$

The incompressible model may be viewed as the formal limit as $\mu \rightarrow +\infty$ of a system with potential $W_0(a) + \mu_3(a_3 - 1)^2$, penalizing variations in density $\det F = a_3$. Operationally, this amounts to fixing $a_3 = 1$ in a given (compressible) elastic potential and dropping the equation for a_3 , to obtain a reduced shear potential $\tilde{W}(a_1, a_2) = W(a_1, a_2, 1)$ and equations whose first-order part have the same variational structure (3.3) as the full 3d system.

3.2.3 The 2D compressible case

Another reduced version of (3.14), restricted to the $v-w$ plane is obtained by setting $u = 0$. This is an equally simple system as (3.15), but with essentially different structure (we now write $|a|^2 = a_2^2 + a_3^2$):

$$(3.17) \quad \begin{aligned} a_{2,t} - b_{2,z} &= 0, & b_{2,t} - (|a|^2 a_2)_z &= \left(\frac{b_{2,z}}{a_3} \right)_z, \\ a_{3,t} - b_{3,z} &= 0, & b_{3,t} - ((|a|^2 - 1)a_3)_z &= 2 \left(\frac{b_{3,z}}{a_3} \right)_z, \end{aligned}$$

while for \mathcal{Z}_1 , writing $a \cdot b_z = a_2 b_{2,z} + a_3 b_{3,z}$, we have:

$$(3.18) \quad \begin{aligned} a_{2,t} - b_{2,z} &= 0, & b_{2,t} - (|a|^2 a_2)_z &= (b_{2,z} + 2a_2 a \cdot b_z)_z, \\ a_{3,t} - b_{3,z} &= 0, & b_{3,t} - ((|a|^2 - 1)a_3)_z &= (2a_3 a \cdot b_z)_z. \end{aligned}$$

3.2.4 The 1D cases

Taking $v = w = 0$, (3.14) further reduces to a model of the transverse unidirectional perturbations in a beam or string:

$$(3.19) \quad a_{1,t} - b_{1,z} = 0, \quad b_{1,t} - (a_1^3 + a_1)_z = b_{1,zz}.$$

Setting $u = v = 0$, (3.14) yields the 1D compressible model for longitudinal perturbations in a viscoelastic rod:

$$(3.20) \quad a_{3,t} - b_{3,z} = 0, \quad b_{3,t} - (a_3^3 - a_3)_z = 2 \left(\frac{b_{3,z}}{a_3} \right)_z.$$

3.2.5 Extension: surface energy and higher-order dispersion

We mention briefly the effects of modifying by the addition of surface energy term. In the planar, incompressible shear case, (2.10) with (2.11) becomes:

$$(3.21) \quad \begin{aligned} a_{1,t} - b_{1,z} &= 0, & b_{1,t} - (a_1 + (a_1^2 + a_2^2)a_1)_z &= b_{1,zz} - a_{1,zzz}, \\ a_{2,t} - b_{2,z} &= 0, & b_{2,t} - (a_2 + (a_1^2 + a_2^2)a_2)_z &= b_{2,zz} - a_{2,zzz}. \end{aligned}$$

See [Sl] for a corresponding treatment of the one-dimensional case.

3.3 Hyperbolic characteristics

3.3.1 Compressible case

Consider the inviscid version of (3.11): $V_t + DG(V)V_z = 0$. Using the block structure of DG in (3.3) we obtain that its eigenvalues are $\{\pm\sqrt{m_j}\}_{j=1}^3$ with corresponding eigenvectors $(\{r_j, \mp\sqrt{m_j}r_j\}_{j=1}^3)$, where m_j (and r_j) are the eigenvalues (and corresponding eigenvectors) of the symmetric matrix M . Also, since m_j are independent of b , the linear degeneracy or genuine nonlinearity of the $\pm\sqrt{m_j}$ characteristic fields of DG is equivalent to the same properties of the m_j characteristic fields of M .

Using now the following formula, valid for 3×3 matrices: $\det(A + B) = \det A + (\text{cof}A) : B + (\text{cof}B) : A + \det B$, we obtain:

$$(3.22) \quad \begin{aligned} m_1 &= |a|^2, \\ m_2 &= \frac{1}{2} \left(4|a|^2 - 1 - \sqrt{(2|a|^2 - 1)^2 + 8(a_1^2 + a_2^2)} \right), \\ m_3 &= \frac{1}{2} \left(4|a|^2 - 1 + \sqrt{(2|a|^2 - 1)^2 + 8(a_1^2 + a_2^2)} \right). \end{aligned}$$

Note that at $a = (0, 0, 1)$ we have $m_1 = m_2 = 1$ and $m_3 = 2$; hence DG is (nonstrictly) hyperbolic at $V_0 = (0, 0, 0, b_1, b_2, b_3)$. Further calculations show that, whenever defined:

- (i) $r_1 = (a_2, -a_1, 0)^T$ and the eigenvalues $\pm\sqrt{m_1}$ correspond to two linearly degenerate fields of DG .
- (ii) $r_2 = (-2a_1a_3, -2a_2a_3, 3|a|^2 - 2a_3^2 - m_2)^T$
- (iii) $r_3 = (-2a_1a_3, -2a_2a_3, 3|a|^2 - 2a_3^2 - m_3)^T$ and in the vicinity of V_0 the eigenvalues $\pm\sqrt{m_3}$ correspond to two genuinely nonlinear fields of DG .

3.3.2 The 2D incompressible shear case

The system (3.15) can be written as:

$$a_t - b_z = 0, \quad b_t - (D_a W(a))_z = b_{zz}.$$

Its flux matrix depends on $a = (a_1, a_2)$ and has the form:

$$(3.23) \quad DG_{1-2} = \begin{pmatrix} 0 & -\text{Id}_2 \\ -M_{1-2} & 0 \end{pmatrix}, \quad M_{1-2} = D_a^2 W_0(a) = (|a|^2 + 1)\text{Id}_2 + 2a \otimes a,$$

where $W_0(a) = \frac{1}{4}|a|^4 + \frac{1}{2}|a|^2$. We see that strict hyperbolicity, convexity of W_0 and existence of strictly convex entropy are equivalently satisfied here.

Calculating as before, DG_{1-2} has two genuinely nonlinear characteristic fields, with eigenvalues $\pm\sqrt{1+3|a|^2}$ and corresponding eigenvectors

$$(\pm a_1, \pm a_2, a_1\sqrt{1+3|a|^2}, a_2\sqrt{1+3|a|^2})^T$$

in fast modes, and two linearly degenerate fields with eigenvalues $\pm\sqrt{1+|a|^2}$ and eigenvectors $(\pm a_2, \mp a_1, a_2\sqrt{1+|a|^2}, -a_1\sqrt{1+|a|^2})^T$ in slow modes. The linear degeneracy reflects the rotational degeneracy of the underlying system [F].

3.3.3 The 2D compressible case

The flux matrix in (3.17) depends on $a = (a_2, a_3)$ and has the form:

$$(3.24) \quad DG_{2-3} = \begin{pmatrix} 0 & -\text{Id}_2 \\ -M_{2-3} & 0 \end{pmatrix}, \quad M_{2-3} = \text{diag}(|a|^2, |a|^2 - 1) + 2a \otimes a,$$

and we find that DG_{2-3} has two couples of eigenvalues $\{\pm\sqrt{m_j}\}_{j=2,3}$ with corresponding eigenvectors $(r_j, \mp\sqrt{m_j}r_j)$, where: $m_2 = \frac{1}{2}\left(4|a|^2 - 1 - \sqrt{(2|a|^2 - 1)^2 + 8a_2^2}\right)$, $m_3 = \frac{1}{2}\left(4|a|^2 - 1 + \sqrt{(2|a|^2 - 1)^2 + 8a_2^2}\right)$, while $r_j = (-2a_2a_3, 3|a|^2 - 2a_3^2 - m_j)^T$ (or $r_2 = (1, 0)^T$ when $a_2 = 0$). We see that in the vicinity of $(0, 1, b_2, b_3)$ the matrix DG_{2-3} is strictly hyperbolic, the two eigenfields corresponding to $\pm\sqrt{m_3}$ are genuinely nonlinear.

3.3.4 The 1D incompressible case

For system (3.19) the characteristic speeds are $\pm\sqrt{1+3a_1^2}$, while for the system (3.20) they are $\pm\sqrt{3a_3^2-1}$. Hence the second model is strictly hyperbolic for $|a_3| > 1/\sqrt{3}$ and elliptic otherwise; this can be recognized as agreeing with certain phase-transitional viscoelasticity models, except that the region $a_3 \leq 0$ (where $\det F \leq 0$) is unphysical.

4 Nonlinear stability framework

We now briefly recall the general stability theory of [Z4, R, RZ], which reduces the question of nonlinear stability in (3.11) to verification of an Evans function condition. Namely, given two endstates V_- and V_+ belonging to the regions of strict hyperbolicity of DG , we make a smooth change of coordinates $V \mapsto S(V)$ with $S: \mathbb{R}^6 \rightarrow \mathbb{R}^6$ given by: $S(V) = D\eta(V) = D_a W(a) \oplus b$. The system (3.11) is equivalent to:

$$\tilde{A}^0(S)S_t + \tilde{A}(S)S_z = (\tilde{B}(S)S_z)_z,$$

where with a slight abuse of notation we use $S = S \circ V : [0, \infty) \times \mathbb{R}^3 \rightarrow \mathbb{R}^{12}$. Above:

$$\tilde{A} = DG(V)\tilde{A}^0 = \begin{bmatrix} 0 & -\text{Id}_3 \\ -MQ & 0 \end{bmatrix}, \quad \tilde{B} = B(V)\tilde{A}^0 = B(V), \quad \tilde{A}^0 = \begin{bmatrix} Q & 0 \\ 0 & \text{Id}_3 \end{bmatrix},$$

where $Q = Q(V)$ is defined as follows. In some open neighborhoods of V_- and V_+ (where M is positive definite) we set $Q = M^{-1}$, in which case:

$$\tilde{A}^0 = \frac{\partial V}{\partial S} = (D_V^2 \eta)^{-1} = \begin{bmatrix} M^{-1} & 0 \\ 0 & \text{Id}_3 \end{bmatrix}.$$

In the region where M is negative definite, we set $Q = \text{Id}_3$. In between the two above mentioned regions, Q is a smooth, symmetric and positive definite interpolation of the two matrix fields M and Id_3 . This construction allows us to treat also the case of profiles passing through elliptic regions, but with hyperbolic endstates (in a similar spirit as for the van der Waals gas dynamics examples mentioned in [MaZ4, Z4]).

We first check the validity of the structural conditions (A1)–(A3) of [Z4]:

(A1) $\tilde{A}(V_-)$ and $\tilde{A}(V_+)$ are symmetric matrices. \tilde{A}_0 is symmetric and positive definite (on the whole \mathbb{R}^6). Also, the 3×3 principal minor of \tilde{A} , corresponding to the purely hyperbolic part of the system (3.11), equals identically 0_3 hence it is always symmetric, as required.

(A2) At the endstates V_\pm there holds: no eigenvector of DG belongs to the kernel of B . In the region of strict hyperbolicity of DG this condition is equivalent to: no eigenvector of M is in the kernel of $B_{0,1}$, readily satisfied.

(A3) \tilde{B} has the required block structure $\tilde{B} = \begin{bmatrix} 0_3 & 0_3 \\ 0_3 & B_0 \end{bmatrix}$ as in (3.12). The symmetrization of the minor corresponding to the parabolic part of the system (3.11): $\text{sym } B_{0,i} = B_{0,i}$ is uniformly elliptic in any region in V of the form: $0 < a_3 < C$ in case of $B_{0,2}$, and $a_3^2 > c(1 + a_1^2 + a_2^2)$ in case of $B_{0,1}$ (where $c, C > 0$ are some uniform constants).

We hence find that shock profiles of each of the planar systems considered in this paper satisfy conditions (A1)–(A3) of [Z4] defining the class of symmetrizable hyperbolic–parabolic systems and profiles to which the theory of nonlinear stability of viscous shock profiles developed in [MaZ2, MaZ3, MaZ4, Z4, R, RZ] applies, provided:

- (i) the endstates V_\pm lie in the region of strict hyperbolicity of DG ,
- (ii) The profile $\{\tilde{V}(\cdot)\}$ lies in some region where the chosen $B_{0,i}$ is uniformly elliptic.

We now validate the additional technical conditions (H0)–(H3) of [Z4]. Note that the remaining conditions (H4)–(H5) are needed only for the multi-dimensional systems, as they automatically hold for systems in 1 space dimension.

(H0) $G, B, S \in \mathcal{C}^5$.

(H1) the shock speed s under consideration is non-zero (note that 0 is the only eigenvalue of the 3×3 principal minor of DG , which indeed is 0_3). As remarked in section 5, $s \neq 0$ for any profile with endstates belonging to the strict hyperbolicity region of DG .

(H2) s is distinct from the eigenvalues of $DG(V_{\pm})$.

(H3) local to $\bar{V}(\cdot)$, the set of traveling wave solutions to (3.11) connecting (V_-, V_+) (with thus determined speed s), forms a smooth finite-dimensional submanifold $\{\bar{V}^{\delta}(\cdot)\}$ of $\mathcal{C}^1(\mathbb{R}, \mathbb{R}^6)$, parametrized by $\delta \in B(0, r) \subset \mathbb{R}^{\ell}$, and $\bar{V}^0 = \bar{V}$.

4.1 The Evans condition

Linearizing the hyperbolic-parabolic system (3.11) about its viscous shock solution of (3.11):

$$V(z, t) = \bar{V}(z - st), \quad \lim_{z \rightarrow \pm\infty} \bar{V}(z) = V_{\pm},$$

which satisfies: $-s\bar{V} + (G(\bar{V}))_z = (B(\bar{V})\bar{V}_z)_z$, and further changing to co-moving coordinates $\tilde{z} = z - st$, we obtain the equivalent evolution equations:

$$(4.1) \quad V_t = \mathcal{L}V := (\mathcal{B}V_z)_z - (\mathcal{G}V)_z.$$

Here \mathcal{G} and \mathcal{B} are the following matrix fields depending on z :

$$\mathcal{G}(z) = DG(\bar{V}(z)) - s\text{Id} - DB(\bar{V}(z))^T \bar{V}_z(z), \quad \mathcal{B}(z) = B(\bar{V}(z)),$$

and converging asymptotically to values $\mathcal{G}(\pm\infty) = DG(V_{\pm}) - s\text{Id}$ and $\mathcal{B}(\pm\infty) = B(V_{\pm})$. Towards investigating stability of (4.1), one seeks eigenvalues $\lambda \in \mathbb{C}$ of \mathcal{L} , that is solutions to the system $\mathcal{L}V = \lambda V$ written in its first-order form:

$$(4.2) \quad Z'(z, \lambda) = \mathcal{A}(z, \lambda)Z(z, \lambda).$$

The augmented ‘‘phase variable’’ Z consists of $V = (a, b)$ and the derivative b' of its parabolic-like component.

As shown in [GZ, ZH, MaZ3, MaZ4, Z4], under conditions (H0), (H1), (H2) it is possible to define an analytic *Evans function* $D : \{\lambda \in \mathbb{C}; \text{Re } \lambda \geq 0\} \rightarrow \mathbb{C}$ associated with (4.2) and hence consequently associated with \mathcal{L} and with the original problem (3.11). We shall now briefly sketch this construction, for further details see e.g. [AGJ, GZ, Z4, HuZ].

In the first step one observes that the complex matrix field $\mathcal{A}(z, \lambda) \in \mathbb{C}^{N \times N}$ in (4.2) is analytic in λ and has an exponential decay to the respective $\mathcal{A}_{\pm}(\lambda)$ as $z \rightarrow \pm\infty$ (uniformly in bounded λ). The second step consists in proving that (4.2) on each of the half-lines $(-\infty, 0]$ and $[0, \infty)$, is equivalent to:

$$\tilde{Z}'(z) = \mathcal{A}_-(\lambda)\tilde{Z}(z), \quad z \leq 0 \quad \text{and} \quad \tilde{Z}'(z) = \mathcal{A}_+(\lambda)\tilde{Z}(z), \quad z \geq 0,$$

under change of variables $Z(z) = P_-(z, \lambda)\tilde{Z}(z)$ for $z \leq 0$, and $Z(z) = P_+(z, \lambda)\tilde{Z}(z)$ for $z \geq 0$. Existence of such (non-unique) analytic in λ and invertible matrix fields $P_{\pm}(z, \lambda) \in \mathbb{C}^{N \times N}$, decaying exponentially to Id as $z \rightarrow \pm\infty$, is achieved by a conjugation lemma [Z4].

Further, denote by $\{\tilde{Z}_i^+(\lambda)\}_{i=1..k}$ the (analytic in λ) basis of the stable space \mathcal{S} of $\mathcal{A}_+(\lambda)$, and likewise let $\{\tilde{Z}_i^-(\lambda)\}_{i=k+1..N}$ be the basis of the unstable space \mathcal{U} of $\mathcal{A}_-(\lambda)$, where the consistency of the dimensions follows from assumptions (H1), (H2). Define:

$$Z_i^+(z, \lambda) = P_+(z, \lambda)\tilde{Z}_i^+(\lambda), \quad z \geq 0 \quad \text{and} \quad Z_i^-(z, \lambda) = P_-(z, \lambda)\tilde{Z}_i^-(\lambda), \quad z \leq 0.$$

Clearly, given any $Z_0 \in \text{span}\{Z_i^+(z_0, \lambda)\}_{i=1..k}$, $z_0 \geq 0$, there exists a solution to (4.2) on $[z_0, \infty)$ decaying exponentially to 0 as $z \rightarrow \infty$, and with initial data $Z(z_0) = Z_0$. It has the property that $Z(z, \lambda) \in \text{span}\{Z_i^+(z, \lambda)\}_{i=1..k}$ for all $z \geq z_0$. A similar assertion of backward resolvability of (4.2) is true for $Z_0 \in \text{span}\{Z_i^-(z_0, \lambda)\}_{i=k+1..N}$, $z_0 \leq 0$ with exponential decay at $z \rightarrow -\infty$.

The Evans function is now introduced as the following Wronskian:

$$(4.3) \quad D(\lambda) = \det \left(Z_1^+(0, \lambda), \dots, Z_k^+(0, \lambda), Z_{k+1}^-(0, \lambda), \dots, Z_N^-(0, \lambda) \right).$$

Away from the origin $\lambda = 0$, D vanishes at λ with $Re \lambda \geq 0$ if and only if λ is an eigenvalue of \mathcal{L} , corresponding to existence of a solution $Z(z, \lambda)$ of $\mathcal{L}Z = \lambda Z$, decaying to 0 at both $z \rightarrow \pm\infty$. Indeed, the multiplicity of the root is equal to the multiplicity of the eigenvalue [GJ1, GJ2, MaZ3, Z4]. The meaning of the multiplicity of the root of D at embedded eigenvalue $\lambda = 0$ is less obvious, but is always greater than or equal to the order of the embedded eigenvalue [MaZ3, Z4].

In agreement with [MaZ3, Z4], we define the *Evans stability condition*:

(D) D has no root in $\{Re \lambda \geq 0\}$ except for $\lambda = 0$, which is the root of multiplicity ℓ .

Note that under assumption (H3), the condition (D) is equivalent to D having precisely ℓ zeros in $\{Re \lambda \geq 0\}$.

4.2 Type of the shock

Define:

$$\begin{aligned} \tilde{\ell} = & \text{dimension of the unstable subspace of } DG(V_-) \\ & + \text{dimension of the stable subspace of } DG(V_+) - \dim V, \end{aligned}$$

where $\dim V = 6$ is the dimension of the whole space. Then, the hyperbolic shock (V_-, V_+) is defined to be:

- (i) of *Lax type* if $\tilde{\ell} = 1$,
- (ii) of *overcompressive type* if $\tilde{\ell} > 1$,
- (iii) of *undercompressive type* if $\tilde{\ell} < 1$.

If $\tilde{\ell} = \ell \geq 1$ or $\tilde{\ell} < \ell = 1$, with ℓ as in (H3), then the viscous shock \bar{V} is defined to be of *pure Lax*, *overcompressive*, or *undercompressive* type, according to the hyperbolic classification just above. Otherwise, \bar{V} is defined as *mixed under-overcompressive type*, [LZu, ZH, MaZ3, Z4]. All the shocks considered in this paper appear to be of pure type. Indeed, though artificial examples are easily constructed [LZu, ZH], we do not know of any physical example of a mixed-type shock.

4.3 Linear and nonlinear stability

Consider a planar viscoelastic shock for which the endstates V_{\pm} lie in the region of strict hyperbolicity and profile $\{\bar{V}(\cdot)\}$ lies in the region for which $B_{0,i}$ is uniformly elliptic.

We have the following basic results relating the Evans condition (D) to stability.

Proposition 4.1 ([MaZ3]). *Assume (H0), (H2) and (H3). The Evans condition (D) is necessary and sufficient for the linearized stability $L^1 \cap L^p \rightarrow L^p$ of \bar{V} , for all $1 \leq p \leq \infty$:*

$$\|e^{t\mathcal{L}}f\|_{L^p} \leq C(\|f\|_{L^1} + \|f\|_{L^p}).$$

Proposition 4.2 ([MaZ4, RZ]). *Assume (H0), (H2), (H3) and (D). Then we have:*

(i) *Stability. For any initial data $\tilde{V}(\cdot, 0)$ with:*

$$E_0 := \|(1 + |z|^2)^{3/4}(\tilde{V}(\cdot, 0) - \bar{V})\|_{H^5} \ll 1$$

sufficiently small, a solution \tilde{V} of (3.11) exists for all $t \geq 0$ and:

$$(4.4) \quad \|(1 + |z|^2)^{3/4}(\tilde{V}(\cdot, t) - \bar{V}(\cdot - st))\|_{H^5} \leq CE_0.$$

(ii) *Phase-asymptotic orbital stability. There exist $\alpha(t)$ and α_∞ such that:*

$$(4.5) \quad \|\tilde{V}(\cdot, t) - \bar{V}^{\alpha(t)}(\cdot - st)\|_{L^p} \leq CE_0(1+t)^{-(1-1/p)/2}$$

and:

$$(4.6) \quad |\alpha(t) - \alpha_\infty| \leq CE_0(1+t)^{-1/2}, \quad |\dot{\alpha}(t)| \leq CE_0(1+t)^{-1},$$

for all $1 \leq p \leq \infty$.

Lemma 4.3. *Assume (H0), (H2) and (D). If $\tilde{\ell} = \ell$ or $\ell = 1$, with ℓ as in (D), then (H3) holds with the same value ℓ . In particular, these conditions together imply nonlinear time-asymptotic orbital stability.*

Proof. The claim follows by the existence theory of [MaZ3], relating the dimensions of stable and unstable manifolds of the rest points V_\pm in the traveling-wave ODE, to the hyperbolic index $\tilde{\ell}$. Further [GZ, ZH, MaZ3], stability condition (D) implies “maximal transversality” consistent with existence of a profile of the traveling-wave connection as a solution of the traveling-wave ODE (i.e. actual transversality), yielding (H3) with $\tilde{\ell} = \ell$ in the case $\tilde{\ell} \geq 1$, and (H3) with $\ell = 1$. ■

Combining Proposition 4.2 with Lemma 4.3, we obtain:

Theorem 4.4. *For each of the planar systems considered in this paper, every viscous Lax, overcompressive, or undercompressive shock satisfying:*

- (i) *condition (H2) (noncharacteristicity),*
- (ii) *with endstates lying in the region of strict hyperbolicity of DG,*
- (iii) *with profile lying in the region of uniform ellipticity of $B_{0,i}$,*
- (iv) *satisfying (D),*

is linearly and nonlinearly orbitally stable.

In particular, Propositions 4.1, 4.2 and Theorem 4.4 apply to profiles with $a \in \mathbb{R}^3$ such that the corresponding F of the form (3.1) is contained in a sufficiently small neighborhood of $SO(3)$. In the incompressible shear case, they apply to any profile with endstates $a_{\pm} \neq 0$.

The condition (H2) corresponds to noncharacteristicity of the shock, which holds generically. It guarantees also exponential decay of the shock to its endstates [MaZ3, Z4], which is needed for efficient numerical approximation of the profile.

Finally, we remark that strict hyperbolicity at V_{\pm} is not necessary for existence of profiles, but only to apply the basic stability framework developed in this section. When hyperbolicity fails, the corresponding endstate is unstable as a constant solution; however, this instability can be stabilized by convective effects if unstable modes are convected sufficiently rapidly into the shock zone; see Appendix C. This situation cannot occur for shear flows, for which all states are hyperbolic, but would be interesting to investigate in the compressible case.

4.4 The integrated Evans condition

Making the substitution $\tilde{V}(z) = \int_{-\infty}^z V(y) dy$ and integrating the equations in (4.2) from $-\infty$ to z , we obtain after dropping the tilde notation:

$$(4.7) \quad \lambda V = \tilde{\mathcal{L}}V := \mathcal{B}V'' - \mathcal{G}V'.$$

We conclude for any $\lambda \neq 0$, satisfaction of (4.2) for a solution V decaying exponentially up to one derivative, implies that $\tilde{V}(z)$ is also exponentially decaying and satisfies (4.7).

Associated with $\tilde{\mathcal{L}}$ is an *integrated Evans function* $\tilde{D}(\lambda)$, which like D is analytically defined on the nonstable half-plane $\{Re \lambda \geq 0\}$, through the construction sketched in section 4.1. In the Lax and overcompressive cases, the change to integrated coordinates has the effect of removing the zeros of D at the origin, making the Evans function easier to compute numerically and hence the stability condition easier to verify.

Proposition 4.5 ([ZH, MaZ3]). *Assume (H0), (H2). Then the Evans condition (D) is equivalent to the following integrated Evans condition:*

(i) *for the Lax and overcompressive shock types:*

(\tilde{D}) *the integrated Evans function \tilde{D} is nonvanishing on $\{Re \lambda \geq 0\}$,*

(ii) *for the undercompressive shock type:*

(\tilde{D}') *the function \tilde{D} has on $\{Re \lambda \geq 0\}$ a single zero of multiplicity $1 + |\tilde{\ell}|$, at $\lambda = 0$.*

Note that the inclusion of term $|\tilde{\ell}|$ repairs an omission in [HLZ], for which $\tilde{\ell} \equiv 0$ in the undercompressive case. Propositions 4.5, 4.4, 4.2 and 4.1 give together a simple and readily numerically evaluated test for stability of large-amplitude and or non-Lax-type waves.

4.5 Small-amplitude stability

The following proposition gives a first nonlinear stability result for planar viscoelastic shocks, answering a conjecture posed in [AM] for the shear wave case.

Proposition 4.6 ([HuZ]). *Assume (H0). Let V_0 be a point of strict hyperbolicity of DG and let λ_0 be one of its eigenvalues, associated with a genuinely nonlinear characteristic field. Then there exists $\epsilon > 0$ sufficiently small such that for any viscous shock \bar{V} with speed s satisfying:*

$$\|\bar{V} - V_0\|_{L^\infty} < \epsilon \quad \text{and} \quad |s - \lambda_0| < \epsilon,$$

we have:

- (i) *the shock is of Lax type,*
- (ii) *the Evans condition (D) holds, hence \bar{V} is linearly and nonlinearly phase-asymptotically orbitally stable.*

5 Existence of viscous shock profiles

Let us now seek traveling waves connecting given endstates:

$$V_- = V(-\infty) = (\alpha, 0), \quad V_+ = V(+\infty) = (a_+, b_+).$$

Indeed, by invariance of (2.1) under change in coordinate frame $\xi \mapsto \xi + b_0 t$, we may without loss of generality assume that $b(-\infty) = 0$.

Hereafter we restrict to the simpler (and apparently more physical) case of viscosity tensor \mathcal{Z}_2 . The case \mathcal{Z}_1 may be treated similarly. We note that the type and location of equilibria of the traveling wave ODE under are assumptions are independent of the choice of \mathcal{Z} , by the general results of [MaZ3]; see [BLZ] for further discussion in the somewhat similar context of MHD.

Writing the profile equation for (3.11) with (2.7) and (2.9), we obtain:

$$(5.1) \quad -sa' - b' = 0, \quad -sb' - DW_0(a)' = \left(\frac{(b'_1, b'_2, 2b'_3)}{a_3} \right)'.$$

Note that $s \neq 0$ for profiles satisfying the nonlinear stability conditions (namely, the endstates belonging to the strict hyperbolicity region of DG). For otherwise $b' = 0$ and $DW_0(a)' = 0$ hence $M(a)a' = 0$ along the profile, contradicting the invertibility of M in the neighborhood of $a(-\infty)$.

Now, substituting the first equation into the second, making the change of variable $z \mapsto sz$, and defining $\sigma = s^2$, we get the following *reduced profile equation*:

$$(5.2) \quad -\sigma a' + DW_0(a)' = \left(\frac{(a'_1, a'_2, 2a'_3)}{a_3} \right)',$$

recognized as associated with the strictly parabolic gradient flux system in a alone:

$$(5.3) \quad a_t + DW_0(a)_z = \left(\frac{(a_1, a_2, 2a_3)_z}{a_3} \right)_z.$$

Note that $\eta(a) = \frac{|a|^2}{2}$ is the convex entropy for (5.2) as:

$$\nabla \eta(a) \cdot D_a^2 W(a) = \nabla q(a), \quad q(a) = a \cdot D_a W(a) - W(a).$$

Evidently, (5.2) may be written as a generalized gradient flow:

$$(5.4) \quad \frac{(a'_1, a'_2, 2a'_3)}{a_3} = \nabla_a \phi(a), \quad \phi(a) = W_0(a) - \sigma \frac{|a|^2}{2} - (DW_0(\alpha) - \sigma \alpha) \cdot a,$$

where $\alpha = a(-\infty)$. Making the change of variable $z \mapsto \tilde{z}(z)$ where \tilde{z} solves the ODE: $\tilde{z}'(z) = 1/a_3(\tilde{z}(z))$, the system (5.4) becomes:

$$(5.5) \quad (a'_1, a'_2, 2a'_3) = \nabla_a \phi(a).$$

We see that the function $z \mapsto \phi(a(z))$ is non-decreasing:

$$(5.6) \quad (\phi \circ a)' = (\nabla \phi) a' = a_3 \operatorname{diag} \left(1, 1, \frac{1}{2} \right) \nabla \phi(a) \otimes \nabla \phi \geq 0$$

in the admissible region $a_3 > 0$. This is a simple instance of a more general fact concerning parabolic conservation laws possessing a viscosity-compatible strictly convex entropy [G, CS1, CS2, BLZ]. Moreover, the type of the shock connection of the original viscoelasticity equations is the same as the type for the reduced equations (5.3), which is in turn determined by the relative Morse index of the endstates/equilibria considered as critical points a :

$$DW_0(a) - \sigma a - (DW_0(\alpha) - \sigma \alpha) = 0$$

of ϕ . See also the general results and discussion of [MaZ3, BLZ].

Finally, a straightforward calculation shows that:

$$(5.7) \quad s\phi(a) = s\eta(V) - (q(V) + \zeta) + \nabla q(V) \cdot \left(G(V) - G(V_-) - s(V - V_-) \right) \\ \text{for } V = (a, b) \text{ with } b = -s(a - \alpha),$$

where the inviscid flux G , entropy η and entropy flux q are as in (3.3) and (3.4). The relation $b = -s(a - \alpha)$ is valid along the profile, and it follows by integrating the first equation in (5.1) from $-\infty$ to z . The vector $\zeta = sDW(\alpha)\alpha - \frac{1}{2}s^3|\alpha|^2$, which is independent of V , can be seen as an adjustment of the entropy flux q , naturally defined up to a constant.

The quantity in the right hand side of (5.7) is related to the dissipative quantity:

$$\psi(V) = -s\eta(V) + q(V)$$

which decreases across any viscous profile connection lying within the region of strict hyperbolicity of the reference hyperbolic-parabolic system and the region of strict convexity of its entropy η (see[BLZ] and references therein):

$$\psi(V_+) - \psi(V_-) < 0.$$

Indeed, by (5.7) and the Rankine-Hugoniot relations, it follows that:

$$\psi(V_-) = -s\phi(\alpha) \quad \text{and} \quad \psi(V_+) = -s\phi(a_+).$$

Thus, in view of (5.6), we conclude that in the present setting ψ is decreases across any viscous profile with positive speed $s > 0$, even one passing the elliptic region. This clarifies somewhat the role of ϕ in the original system.

5.1 The 3D compressible system

Recalling (3.5), (5.5) becomes:

$$(5.8) \quad \begin{aligned} a'_1 &= (|a|^2 - \sigma)a_1 - (|\alpha|^2 - \sigma)\alpha_1, \\ a'_2 &= (|a|^2 - \sigma)a_2 - (|\alpha|^2 - \sigma)\alpha_2, \\ 2a'_3 &= (|a|^2 - 1 - \sigma)a_3 - (|\alpha|^2 - 1 - \sigma)\alpha_3. \end{aligned}$$

As $|a| \rightarrow \infty$, $\phi(a) \sim \frac{|a|^4}{4}$, hence the phase portrait of (5.4) always possesses a minimum, or repeller. More, $\nabla\phi(a) \sim |a|^2 a$ points in the outward radial direction, and hence the index of this vector field on a suitably large ball is $+1$, and it must be equal to the sum of the indices of the equilibria (generically five - see Section 5.4 and Figure 2), defined as the signs of the associated Jacobians $\text{sgn det}(D^2W_0 - \sigma\text{Id})$. The same argument shows that a sufficiently large ball is absorbing in backwards z , so that we can conclude that any orbit lying in the stable manifold of an equilibrium must connect in backward z to some other equilibrium possessing an unstable manifold.

Further, when $a_3 = 0$ we have $\partial_3\phi = -(|\alpha|^2 - 1 - s^2)\alpha_3$, which is independent of (a_1, a_2) . Since $\nabla\phi \sim |a|^2 a$ as $|a| \rightarrow +\infty$, it follows that the index of $\nabla\phi$ on a large half-ball: $B_R(0) \cap \{a_3 > 0\}$ equals $+1$ for $(|\alpha|^2 - 1 - \sigma)\alpha_3 > 0$, and it equals 0 for $(|\alpha|^2 - 1 - \sigma)\alpha_3 < 0$. In the former case, the region $B_R(0) \cap \{a_3 > 0\}$ is invariant in backward z and so we may conclude that any orbit lying in the stable manifold of an equilibrium in $\{a_3 > 0\}$ must connect in backward z to some other equilibrium in $\{a_3 > 0\}$ possessing an unstable manifold.

5.2 The 2D incompressible shear case

The incompressible case can be analyzed similarly as above, with (5.3) becoming:

$$a_t + DW_0(a)_z = a_{zz},$$

where $a = (a_1, a_2)$ and $W_0(a) = \frac{1}{4}|a|^4 + \frac{1}{2}|a|^2$. That gives a 2×2 rotationally symmetric model:

$$(5.9) \quad a_t + (|a|^2 + 1)a_z = a_{zz},$$

of a form $a_t + (h(|a|)a)_z = a_{zz}$ that has been much studied as a prototypical example of a system with rotational degeneracy [F]. Further, the counterpart of (5.4) reads:

$$a' = \nabla_a \phi(a), \quad \phi(a) = W_0(a) - \sigma \frac{|a|^2}{2} - (DW_0(a) - \sigma a) \cdot a.$$

Expanded in coordinate form, the profile ODE reads:

$$\begin{aligned} a'_1 &= (|a|^2 + 1 - \sigma)a_1 - (|\alpha|^2 + 1 - \sigma)\alpha_1, \\ a'_2 &= (|a|^2 + 1 - \sigma)a_2 - (|\alpha|^2 + 1 - \sigma)\alpha_2. \end{aligned}$$

Again, we find by an asymptotic development of ϕ that the vector index of this ODE on a suitably large ball is $+1$, and there exists always at least one repeller, with index $+1$. In the generic case (see below), there are three nondegenerate equilibria, each of index ± 1 : one is of index $+1$ and of one index -1 .

Writing $\alpha = a(-\infty)$ and $a_+ = a(+\infty)$, the Rankine–Hugoniot relations for (5.9) are:

$$(5.10) \quad (|a_+|^2 + 1 - \sigma)a_+ - (|\alpha|^2 + 1 - \sigma)\alpha = 0.$$

By rotation invariance, we may restrict our attention to $\alpha = (\alpha_1, 0)$. We shall distinguish two cases.

Case (i) $\alpha_1 = 0$. We find that there is a circle of solutions a_+ to (5.10), given by $|a_+|^2 = \sigma - 1$, surrounding the rest state $a_+ = 0$ at the center. Along each radius of the circle, there is a viscous shock connection $a(t, z) = \rho(z - \sigma t)e^{i\theta}$ solution to (5.9) whose norm $\rho = |a|$ satisfies:

$$(5.11) \quad \rho_t + (\rho^3 + \rho)_z = \rho_{zz}$$

and connects $\rho_+ = \rho(+\infty) = \sqrt{\sigma - 1}$ to $\rho_- = \rho(-\infty) = 0$. Note that (5.11) is also the associated parabolic equation to the flow:

$$a'_1 = (a_1^2 + 1 - \sigma)a_1 - (\alpha^2 + 1 - \sigma)\alpha,$$

which is the counterpart of (5.4) for the 1d incompressible model (3.19). When $\alpha_1 = a_1(-\infty) = 0$ then $a_{1+} = a_1(+\infty) = \sqrt{\sigma - 1}$ and thus we obtain:

$$a'_1 = (a_1^2 - \alpha_1^2)a_1,$$

which has the explicit solution:

$$(5.12) \quad a_1(z) = \frac{\alpha_1 \exp(-\alpha_1^2 z)}{\sqrt{k + \exp(-2\alpha_1^2 z)}}$$

with $k > 0$. Note that this solution connects $a(-\infty) = \sqrt{\sigma - 1}$ to $a(+\infty) = 0$; that is, the connection goes in opposite direction from the one sought. Setting now $a(t, z) = a_1(z - \sigma t)e^{i\theta}$ (with constant rotation angle θ) gives the traveling viscous shock solution to (5.9).

Remark 5.1. *Though noncharacteristic when considered as one-dimensional solutions, as reflected by uniform exponential convergence to their endstates (see discussion below Theorem 4.4), such shocks are always characteristic with respect to the transverse (rotational) modes, which have characteristic speeds $\pm\sqrt{|a|^2+1}$ equal to $\pm\sqrt{\sigma} = \pm s$.*

Case (ii) $\alpha_1 \neq 0$. When $a_{2+} = 0$ then (5.10) reduces to $(a_{1+}^2+1-\sigma)a_{1+} = (\alpha_1^2+1-\sigma)\alpha_1$ corresponding to the associated scalar equation (5.11).

When $a_{2+} \neq 0$ then the second equation in (5.10) becomes $a_{1+}^2 + a_{2+}^2 = |a_+|^2 = \sigma - 1$ whence, from the first equation: $\alpha_1^2 = |a|^2 = \sigma - 1$. That is, solutions with $a_{2+} \neq 0$ exist only if σ is equal to the linearly degenerate characteristic speed, which has no profile.

Thus we may without loss of generality restrict to the (at most) triples of possible rest states $(\alpha_1^{(i)}, 0)$ with (to fix the ideas):

$$\alpha_1^{(3)} < 0 < \alpha_1^{(2)} < \alpha_1^{(1)}$$

and $((\alpha_1^{(i)})^2 + 1 - \sigma)\alpha_1^{(i)} < 0$ sufficiently small. Considering the equation (5.11), we find that the outermost rest points $(\alpha_1^{(3)}, 0)$ and $(\alpha_1^{(1)}, 0)$ are connected to the innermost $(\alpha_1^{(2)}, 0)$ by a scalar (1d) shock profile. Indeed:

- $(\alpha_1^{(1)})^2 + 1 - \sigma < 0 < 3(\alpha_1^{(1)})^2 + 1 - \sigma$, so $(\alpha_1^{(1)}, 0)$ is a saddle,
- $(\alpha_1^{(2)})^2 + 1 - \sigma < 3(\alpha_1^{(2)})^2 + 1 - \sigma < 0$, so $(\alpha_1^{(2)}, 0)$ is an attractor,
- $3(\alpha_1^{(3)})^2 + 1 - \sigma > (\alpha_1^{(3)})^2 + 1 - \sigma > 0$, so $(\alpha_1^{(3)}, 0)$ is a repeller.

The phase portrait thus consists of a family of overcompressive profiles connecting $(\alpha_1^{(3)}, 0)$ and $(\alpha_1^{(2)}, 0)$, bounded by Lax shocks between $(\alpha_1^{(3)}, 0)$ and $(\alpha_1^{(1)}, 0)$, and between $(\alpha_1^{(1)}, 0)$ and $(\alpha_1^{(2)}, 0)$, similarly as for the closely related ‘‘cubic model’’ studied, e.g., in [F, Br]. See Figure 1 for typical phase portraits computed numerically using MATLAB.

5.3 The 2D compressible case

Here (5.3) simplifies to:

$$(5.13) \quad \begin{aligned} a_{2,t} + (|a|^2 a_2)_z &= \left(\frac{a_{2,z}}{a_3} \right)_z, \\ a_{3,t} + (|a|^2 - 1)a_{3,z} &= 2 \left(\frac{a_{3,z}}{a_3} \right)_z, \end{aligned}$$

where $a = (a_2, a_3)$ and Rankine–Hugoniot relations are:

$$(5.14) \quad \begin{aligned} (|a_+|^2 - \sigma)a_{2+} - (|a|^2 - \sigma)\alpha_2 &= 0 \\ (|a_+|^2 - 1 - \sigma)a_{3+} - (|a|^2 - 1 - \sigma)\alpha_3 &= 0, \end{aligned}$$

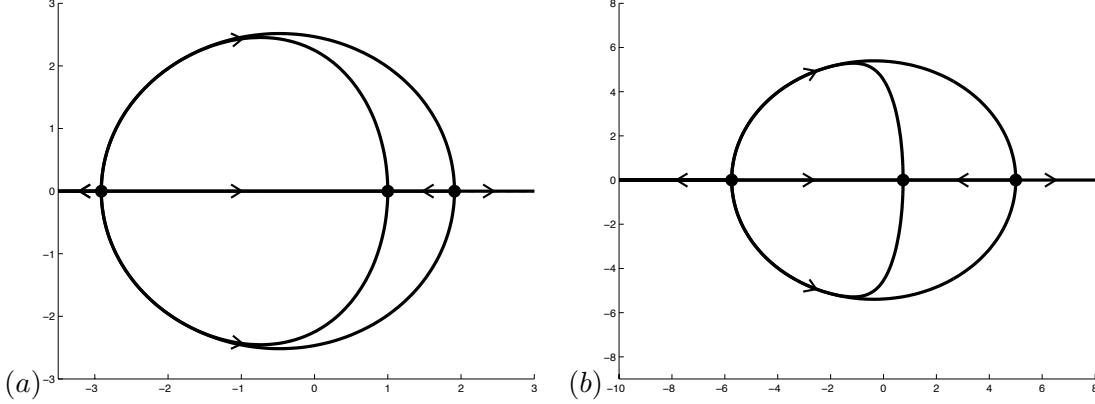


Figure 1: Typical phase portrait for the 2D shear case. In (a) we have $\alpha_1 = 1$ and $\sigma = 11/4$, and in (b) we have $\alpha_1 = 5$ and $\sigma = 121/4$.

where $\alpha = (\alpha_2, \alpha_3) = a(-\infty)$, $a_+ = (a_{2+}, a_{3+}) = a(+\infty)$ and $a_{3+}, \alpha_3 > 0$. We shall distinguish two cases.

Case (i) $\alpha_2 = 0$. Strict hyperbolicity of (3.24) enforces that $\alpha_3 > 1/\sqrt{3}$ and $\alpha_3 \neq 1/\sqrt{2}$. When $a_{2+} = 0$ then (5.14) implies that:

$$a_{3+} = -\frac{1}{2}\alpha_3 \pm \frac{1}{2}\sqrt{4(1+\sigma) - 3\alpha_3^2},$$

with at most one physically feasible solution $a_{3+} > 0$. For every α_3 the range of σ , for which $a_{3+} > 1/\sqrt{3}$ and $a_{3+} \neq 1/\sqrt{2}$ is:

$$\sigma \in \left(\alpha_3^2 + \frac{1}{\sqrt{3}}\alpha_3 - \frac{2}{3}, +\infty\right) \setminus \left\{\alpha_3^2 + \frac{1}{\sqrt{2}}\alpha_3 - \frac{1}{2}\right\}.$$

An associated 1d traveling wave of the type $(0, a_3(z))$ must satisfy:

$$-\sigma a_3' + (a_3^3 - a_3)' = 2 \left(\frac{a_3'}{a_3}\right)'$$

If $a_{2+} \neq 0$, then the first equation in (5.14) implies $|a_+|^2 = \sigma$, while by the second equation: $a_{3+} = (1 + \sigma - \alpha_3^2)\alpha_3$, hence:

$$a_{2+} = \pm \sqrt{\sigma - (1 + \sigma - \alpha_3^2)^2 \alpha_3^2}.$$

We see that there is a pattern of at most four physically feasible equilibria, corresponding to two 1d solutions plus two more symmetrically disposed about the a_3 axis. There are at most five equilibria in total, counting a fifth possible infeasible radial solution with $a_3 < 0$. Here, we are ignoring the line of nonphysical equilibria $a_3 = 0$ induced by the form of the viscosity tensor. See Figures 2 (a) (c) for a typical phase portrait computed numerically using MATLAB.

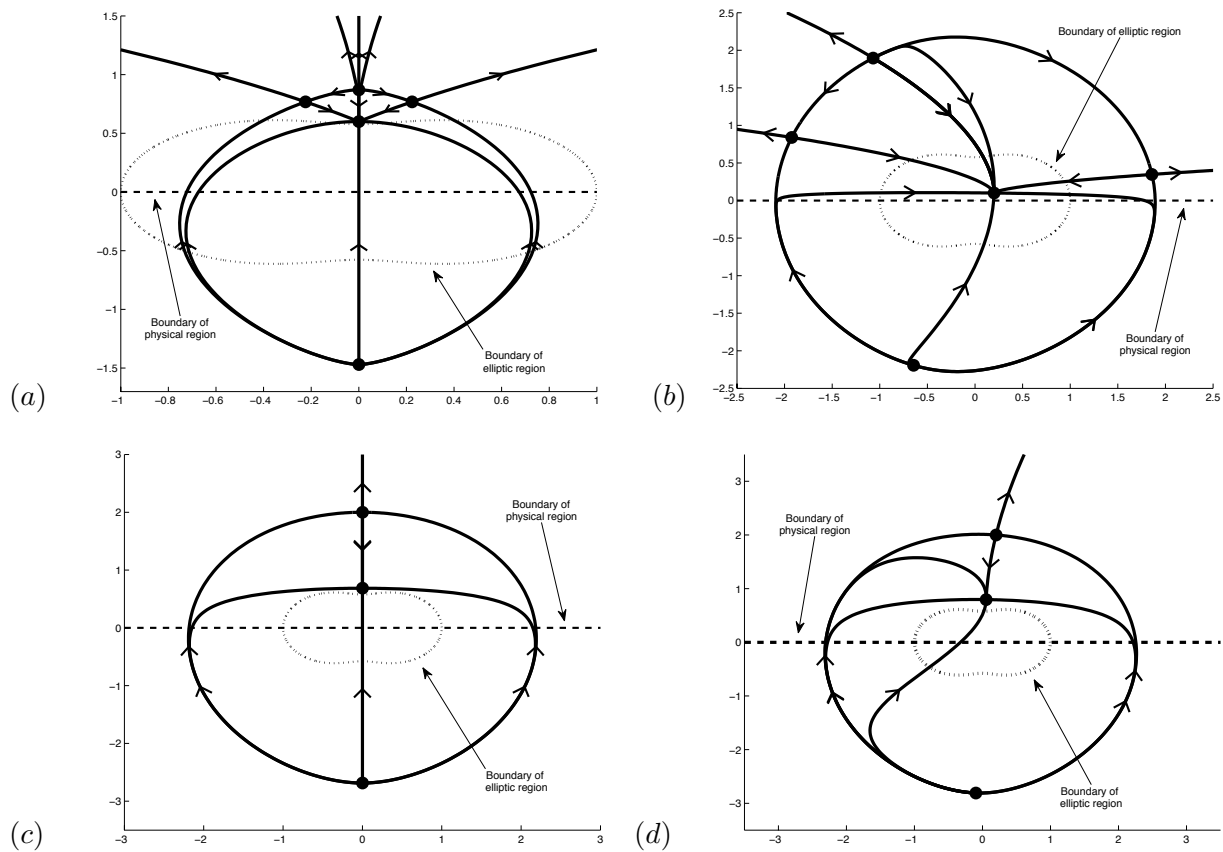


Figure 2: Typical three and five-equilibrium phase portraits for the 2D compressible case. The dark dashed lines bound the physically relevant region $a_3 > 0$ and the light dashed lines surround the region $m_2 < 0$ where the system (3.17) loses hyperbolicity, see Section 3.3.3. In (a) we have $\alpha_2 = 0$, $\alpha_3 = 0.6$, and $\sigma = 0.64$, in (b) $\alpha_2 = 0.2$, $\alpha_3 = 0.1$, and $\sigma = 4$, in (c) $\alpha_2 = 0$, $\alpha_3 = 2$, $\sigma = 4.84$, and in (d) $\alpha_2 = 0.2$, $\alpha_3 = 2$, $\sigma = 5.29$.

Case (ii) $\alpha_2 \neq 0$. Setting $x = |a_+|^2 - |\alpha|^2$ we see that (5.14) is solved by:

$$a_{2+} = \frac{(|\alpha|^2 - \sigma)}{(x + |\alpha|^2 - \sigma)} \alpha_2, \quad a_{3+} = \frac{(|\alpha|^2 - 1 - \sigma)}{(x + |\alpha|^2 - 1 - \sigma)} \alpha_3.$$

Substituting into the definition of x and rearranging we obtain:

$$(5.15) \quad (x + |\alpha|^2)(x + |\alpha|^2 - \sigma)^2(x + |\alpha|^2 - 1 - \sigma)^2 = (|\alpha|^2 - \sigma)^2(x + |\alpha|^2 - 1 - \sigma)^2 \alpha_2^2 + (x + |\alpha|^2 - \sigma)^2(|\alpha|^2 - 1 - \sigma)^2 \alpha_3^2,$$

yielding the quintic:

$$(5.16) \quad y(y - \sigma)^2(y - 1 - \sigma)^2 = (|\alpha|^2 - \sigma)^2(y - 1 - \sigma)^2 \alpha_2^2 + (y - \sigma)^2(|\alpha|^2 - 1 - \sigma)^2 \alpha_3^2,$$

where $y = |a_+|^2$. From the roots of (5.16) a_+ may be recovered through:

$$(5.17) \quad a_{2+} = \frac{|\alpha|^2 - \sigma}{y - \sigma} \alpha_2, \quad a_{3+} = \frac{|\alpha|^2 - 1 - \sigma}{y - 1 - \sigma} \alpha_3.$$

Evidently, these solutions are not 1d, as $a_{2+}/a_{3+} \neq \alpha_2/\alpha_3$, unless $y = |\alpha|^2$, in which case other roots of (5.16) are: $\sigma, 1 + \sigma$, contradicting (5.17).

Recall that the nonphysical solutions with $a_{3+} \leq 0$ are discarded and that the further condition of hyperbolicity of endstates is not necessary for existence of profiles, but is needed to apply the basic stability framework of Section 4. We shall discuss profiles with nonhyperbolic endstates in Appendix C. See Figures 2 (b) (d) for a typical phase portrait computed numerically using MATLAB.

5.4 The 3D compressible case - continued

In the full 3D compressible case, (5.3) can be written as:

$$\begin{aligned} \tilde{a}_t + (|a|^2 \tilde{a})_z &= \begin{pmatrix} \tilde{a}_z \\ a_3 \end{pmatrix}_z, \\ a_{3,t} + ((|a|^2 - 1)a_3)_z &= 2 \begin{pmatrix} a_{3,z} \\ a_3 \end{pmatrix}_z, \end{aligned}$$

with $a = (\tilde{a}, a_3)$ and $\tilde{a} = (a_1, a_2)$. The corresponding Rankine–Hugoniot relations read:

$$(5.18) \quad \begin{aligned} (|a_+|^2 - \sigma)\tilde{a}_+ - (|\alpha|^2 - \sigma)\tilde{\alpha} &= 0 \\ (|a_+|^2 - 1 - \sigma)a_{3+} - (|\alpha|^2 - 1 - \sigma)\alpha_3 &= 0 \end{aligned}$$

where $\alpha = (\tilde{\alpha}, \alpha_3) = a(-\infty)$ and $a_+ = (\tilde{a}_+, a_{3+}) = a(+\infty)$ and $a_{3+}, \alpha_3 > 0$. Also, by invariance with respect to rotations in the \tilde{a} plane, we will assume that $\alpha_1 = 0$, without loss of generality.

Case (i) $\alpha_2 = 0$. Here, the phase portrait can be easily deduced from that in (i) Section 5.3 of the 2d compressible case. That is, there is at most one physically feasible 1d profile connecting to rest point $a_+ = (0, 0, (-\alpha_3 + \sqrt{4(1 + \sigma) - 3\alpha_3^2})/2)$, and a ring of rest points $a_+ = (r \cos \theta, r \sin \theta, a_{3+})$ with $a_{3+} = (1 + \sigma - \alpha_3^2)\alpha_3$ and $r = \pm\sqrt{\sigma - a_{3+}^2}$. Again, we are ignoring possible equilibria in the nonphysical plane $a_3 = 0$.

Case (ii) $\alpha_2 \neq 0$. This case includes the 2d portrait of case (ii) in Section 5.3 for the 2D compressible case when $a_1 \equiv 0$.

If $a_{1+} \neq 0$, then $|a_+|^2 = \sigma$, and so $|\alpha_2|^2 = \sigma$ (in view of the second equation in (5.18)). Thus, except in this degenerate case, the set of equilibria is *only* that of the planar case already treated. The types of shock connections may be different than in Section 5.3, and profiles may go out of plane to yield new connections.

The above situation is quite reminiscent of the case of MHD [BLZ]. In particular, if α_2 is varied slightly from the rotationally symmetric situation $\alpha_2 = 0$, then one may conclude by persistence of invariant sets as in [FS] that ‘‘Alfven’’-type profiles must arise in the rotationally degenerate characteristic field.

6 Numerical stability analysis

In this section, we describe the numerical Evans function method, based on the numerical approximation using the polar-coordinate algorithm developed in [HuZ]; see also [BHRZ, HLZ, HLYZ, BHZ]. Since the Evans function is analytic in the region $\{Re\lambda \geq 0\}$ of interest, we can numerically compute its winding number around a large semicircle $B(0, R) \cap \{Re\lambda \geq 0\}$, enclosing all possible nonstable roots. This allows us to determine stability through the Evans condition (D); alternatively, as we shall do here, through its integrated version (\tilde{D}) (resp., (\tilde{D}')). In the case of instability, one may go further to locate the roots and study stability and bifurcation boundaries as model parameters are varied. This approach was introduced in basic form by Evans and Feroe [EF] and it has since been elaborated and greatly generalized. For applications to successively more complicated systems, see for example [PSW, AS, Br, BrZ, BDG, HuZ, HLZ, HLYZ, BHZ, BLZ].

6.1 The Evans systems

Linearizing about a traveling wave solution $(\bar{a}, \bar{b}) = (\bar{a}_1, \bar{a}_2, \bar{a}_3, \bar{b}_1, \bar{b}_2, \bar{b}_3)$ of (3.14), we obtain the eigenvalue problem:

$$\begin{aligned}
 \lambda a_j - s a'_j - b'_j &= 0 & \text{for } j = 1, 2 \\
 \lambda a_3 - s a'_3 - b'_3 &= 0 \\
 \lambda b_j - s b'_j - (|\bar{a}|^2 a_j + 2(\bar{a} \cdot a) \bar{a}_j)' &= (b'_j / \bar{a}_3 - a_3 \bar{b}'_j / \bar{a}_3^2)' \\
 \lambda b_3 - s b'_3 - (|\bar{a}|^2 - 1) a_3 + 2(\bar{a} \cdot a) \bar{a}_3 &' = 2(b'_3 / \bar{a}_3 - a_3 \bar{b}'_3 / \bar{a}_3^2)'.
 \end{aligned}
 \tag{6.1}$$

We make the substitution $\tilde{a}_i(z) = \int_{-\infty}^z a_i(y) dy$ and $\tilde{b}_i(z) = \int_{-\infty}^z b_i(y) dy$ into (6.1) and then integrate from $-\infty$ to z to obtain, after dropping the tilde notation:

$$(6.2) \quad \begin{aligned} \lambda a_j - s a'_j - b'_j &= 0 \\ \lambda a_3 - s a'_3 - b'_3 &= 0 \\ \lambda b_j - s b'_j - (|\bar{a}|^2 a'_j + 2(\bar{a} \cdot a') \bar{a}_j) &= b''_j / \bar{a}_3 - a'_3 \bar{b}'_j / \bar{a}_3^2 \\ \lambda b_3 - s b'_3 - (|\bar{a}|^2 - 1) a'_3 + 2(\bar{a} \cdot a') \bar{a}_3 &= 2(b''_3 / \bar{a}_3 - a'_3 \bar{b}'_3 / \bar{a}_3^2). \end{aligned}$$

6.1.1 The 3D compressible case

In the full 3D case (6.2) may be written as a first order system $Z' = \mathcal{A}(z, \lambda)Z$, with

$$Z = (b_1, a_1, a'_1, b_2, a_2, a'_2, b_3, a_3, a'_3)^T$$

and

$$(6.3) \quad \mathcal{A}(z, \lambda) = \begin{bmatrix} B(z, \lambda) & C(z, \lambda) \\ D(z, \lambda) & E(z, \lambda) \end{bmatrix},$$

where:

$$(6.4) \quad \begin{aligned} B(z, \lambda) &= \begin{bmatrix} 0 & \lambda & -s \\ 0 & 0 & 1 \\ \frac{-\lambda \bar{a}_3}{s} & \lambda \bar{a}_3 & \frac{\lambda + \bar{a}_3(|\bar{a}|^2 - s^2 + 2\bar{a}_1^2)}{s} \end{bmatrix}, \\ C(z, \lambda) &= \begin{bmatrix} 0 & 0 & 0 & 0 & 0 & 0 \\ 0 & 0 & 0 & 0 & 0 & 0 \\ 0 & 0 & \frac{2\bar{a}_1 \bar{a}_2 \bar{a}_3}{s} & 0 & 0 & \frac{2\bar{a}_1 \bar{a}_3^3 - \bar{b}'_1}{s \bar{a}_3} \end{bmatrix}, \\ D(z, \lambda) &= \begin{bmatrix} 0 & 0 & 0 & 0 & 0 & 0 \\ 0 & 0 & 0 & 0 & 0 & 0 \\ 0 & 0 & \frac{2\bar{a}_1 \bar{a}_2 \bar{a}_3}{s} & 0 & 0 & \frac{\bar{a}_1 \bar{a}_3^2}{s} \end{bmatrix}^T, \end{aligned}$$

$$(6.5) \quad E(z, \lambda) = \begin{bmatrix} 0 & \lambda & -s & 0 & 0 & 0 \\ 0 & 0 & 1 & 0 & 0 & 0 \\ \frac{-\lambda\bar{a}_3}{s} & \lambda\bar{a}_3 & \frac{\lambda + \bar{a}_3(|\bar{a}|^2 - s^2 + 2\bar{a}_2^2)}{s} & 0 & 0 & \frac{-\bar{b}'_2 + 2\bar{a}_2\bar{a}_3^3}{s\bar{a}_3} \\ 0 & 0 & 0 & 0 & \lambda & -s \\ 0 & 0 & 0 & 0 & 0 & 1 \\ 0 & 0 & \frac{\bar{a}_2\bar{a}_3^2}{s} & \frac{-\lambda\bar{a}_3}{2s} & \frac{\lambda\bar{a}_3}{2} & \frac{\bar{a}_3^2(|\bar{a}|^2 - 1 - s^2 + 2\bar{a}_2^2) - 2\bar{b}'_3 + 2\bar{a}_3\lambda}{2s\bar{a}_3} \end{bmatrix}.$$

6.1.2 The 2D incompressible shear case

For (3.15), the same procedure as in (6.1) yields:

$$(6.6) \quad \begin{aligned} \lambda a - sa' - b' &= 0, \\ \lambda b - sb' - ((1 + |\bar{a}|^2)a + 2(\bar{a} \cdot a)\bar{a})' &= b''. \end{aligned}$$

Substituting $\tilde{a}_i(z) = \int_{-\infty}^z a_i(x) dx$, $\tilde{b}_i(z) = \int_{-\infty}^z b_i(y) dy$, into (6.6) and integrating from $-\infty$ to z we obtain, after dropping the tilde notation:

$$(6.7) \quad \begin{aligned} \lambda a_i - sa'_i - b'_i &= 0, \quad \text{for } i = 1, 2 \\ \lambda b_i - sb'_i - ((1 + |\bar{a}|^2)a'_i + 2(\bar{a} \cdot a')\bar{a}_i) &= b''_i. \end{aligned}$$

Let $Z = (a_1, b_1, b'_1, a_2, b_2, b'_2)^T$. Then (6.7) may be written as (4.2), where:

$$\mathcal{A}(z, \lambda) = \begin{bmatrix} \frac{\lambda}{s} & 0 & \frac{-1}{s} & 0 & 0 & 0 \\ 0 & 0 & 1 & 0 & 0 & 0 \\ \frac{-\lambda(1 + 3\bar{a}_1^2 + \bar{a}_2^2)}{s} & \lambda & \frac{1 - s^2 + 3\bar{a}_1^2 + \bar{a}_2^2}{s} & \frac{-2\lambda\bar{a}_1\bar{a}_2}{s} & 0 & \frac{2\bar{a}_1\bar{a}_2}{s} \\ 0 & 0 & 0 & \frac{\lambda}{s} & 0 & \frac{-1}{s} \\ 0 & 0 & 0 & 0 & 0 & 1 \\ \frac{2\lambda\bar{a}_1\bar{a}_2}{s} & 0 & \frac{2\bar{a}_1\bar{a}_2}{s} & \frac{-\lambda(1 + \bar{a}_1^2 + 3\bar{a}_2^2)}{s} & \lambda & \frac{1 - s^2 + \bar{a}_1^2 + 3\bar{a}_2^2}{s} \end{bmatrix}.$$

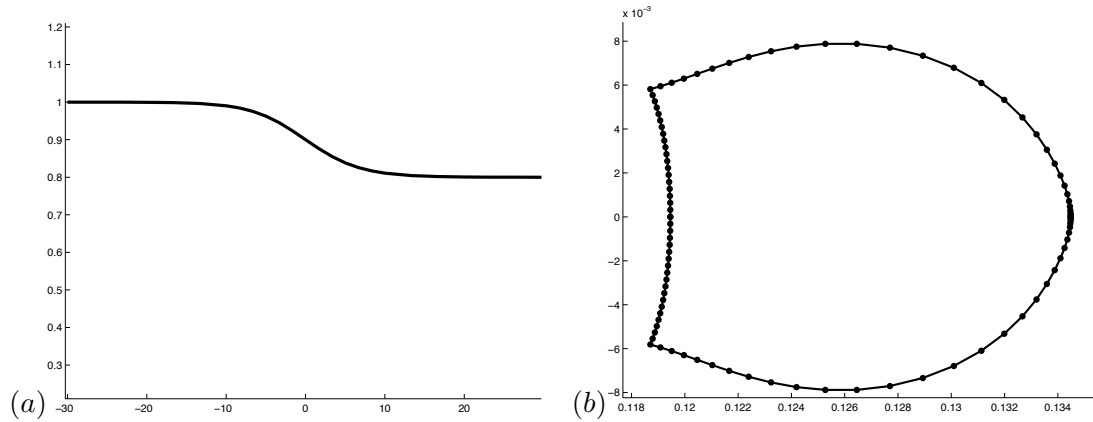


Figure 3: (a) Traveling wave profile \bar{V} for the shear case with parameter values $\alpha_1 = 1$, $\alpha_2 = 0$, and $s = 1.8547$ corresponding to a Lax shock connecting endstates $(1, 0)$ and $(0.8, 0)$. (b) The image of the semicircle under Evans function \tilde{D} .

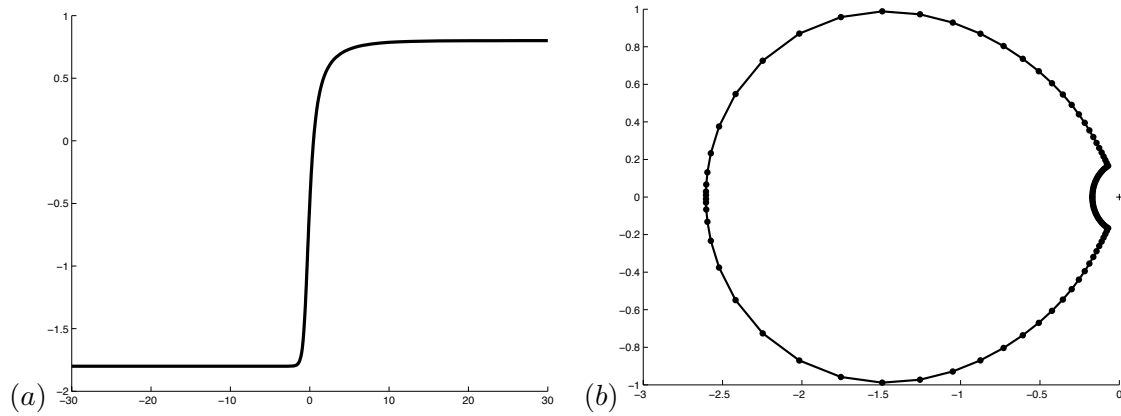


Figure 4: (a) Traveling wave profile \bar{V} for the shear case with parameter values $\alpha_1 = 1$, $\alpha_2 = 0$, $s = 1.8547$ corresponding to an overcompressive wave connecting endstates $(0.8, 0)$ and $(-1.8, 0)$. (b) The image of the semicircle under Evans function \tilde{D} .

6.1.3 The 2D compressible case

With $j = 2$ in (6.2) and using $b'_j = \lambda a_j - s a'_j$, (6.2) can be equivalently written as (4.2) with $Z = (b_2, a_2, a'_2, b_3, a_3, a'_3)^T$ and $\mathcal{A}(z, \lambda) = E(z, \lambda)$ given in (6.5) where $a = (a_2, a_3)$.

6.1.4 Transverse equations

Consider now a 2D compressible solution as a solution of the full 3D system (3.14). We find that the integrated eigenvalue equations (6.2) decouple into the 2D equations plus the transverse system, obtained from the equations corresponding to $j = 1$ in system (6.2) after putting $\bar{a}_1 = \bar{b}_1 = 0$:

$$(6.8) \quad \begin{aligned} \lambda a_1 - s a_1' - b_1' &= 0, \\ \lambda b_1 - s b_1' - |\bar{a}|^2 a_1' &= \frac{b_1''}{\bar{a}_3}, \end{aligned}$$

The system (6.8) has the form of as (4.2) with $Z = (b_1, a_1, a_1')$ and $\mathcal{A}(z, \lambda) = B(z, \lambda)$ given in (6.4), after putting $\bar{a}_1 = 0$.

6.2 Approximation of the profile and of the Evans function

Following [BHRZ, HLZ], we approximate the traveling wave profile using one of MATLAB's boundary-value solvers `bvp4c` [SGT], `bvp5c` [KL], or `bvp6c` [HM]. These are adaptive Lobatto quadrature schemes that can be interchanged for our purposes; for rigorous error/convergence bounds for such algorithms, see e.g. [Be1, Be2]. The calculations are performed on a finite computational domain $[-L, L]$, where the values of approximate plus and minus spatial infinity L are determined experimentally by the requirement that the absolute error $|\bar{V}(\pm L) - V_{\pm}| \leq TOL$ be within a prescribed tolerance, say $TOL = 10^{-3}$. Here \bar{V} and V_{\pm} are the profile and limiting endstates as defined in Section 4.1.

Using now the notation of section 4.1, define for $z \geq 0$ and $z \leq 0$, respectively:

$$\mathcal{Z}^+(z, \lambda) = Z_1^+(z, \lambda) \wedge \dots \wedge Z_k^+(z, \lambda) \quad \text{and} \quad \mathcal{Z}^-(z, \lambda) = Z_{k+1}^-(z, \lambda) \wedge \dots \wedge Z_N^-(z, \lambda),$$

so that the Evans function is given by:

$$(6.9) \quad D(\lambda) = \mathcal{Z}^+(0, \lambda) \wedge \mathcal{Z}^-(0, \lambda).$$

Since for $L > 0$ large, $P_{\pm}(\pm L, \lambda)$ approximately equals Id, we obtain:

$$(6.10) \quad Z_i^{\pm}(\pm L, \lambda) \sim e^{\pm \mathcal{A}_{\pm}(\lambda)L} \tilde{Z}_i^{\pm}(\lambda),$$

where the “+” sign is taken with indices $i = 1 \dots k$ and the “-” sign with $i = k + 1 \dots N$. Recall that $\mathcal{S}(\lambda) = \text{span}\{\tilde{Z}_i^+(\lambda)\}_{i=1..k}$ is the stable space of $\mathcal{A}_+(\lambda)$, while $\mathcal{U}(\lambda) = \text{span}\{\tilde{Z}_i^-(\lambda)\}_{i=k+1..N}$ represents the unstable space of $\mathcal{A}_-(\lambda)$.

The analytic bases $\{\tilde{Z}_i^{\pm}(\lambda)\}_i$ are obtained by the following procedure [HuZ, Z2]. First, one computes the eigenprojections $\mathcal{P}_+(\lambda)$ and $\mathcal{P}_-(\lambda)$ onto, respectively, the space $\mathcal{S}(\lambda)$ and $\mathcal{U}(\lambda)$. This can be done by setting:

$$\mathcal{P}_{\pm} = R_{\pm} (L_{\pm} R_{\pm})^{-1} L_{\pm},$$

where $R_{\pm}(\lambda)$ and $L_{\pm}(\lambda)$ are matrices consisting of any orthonormal right and left bases of $\mathcal{S}(\lambda)$ (when with subscript “+”) and $\mathcal{U}(\lambda)$ (when with subscript “-”). Then, a standard result in matrix perturbation theory [K] states that the analytic in λ bases $\tilde{\mathcal{Z}}^{\pm}(\lambda)$ can be prescribed constructively as the solution of Kato’s ODE:

$$(\tilde{\mathcal{Z}}^{\pm})' = \left(\mathcal{P}'_{\pm} \mathcal{P}_{\pm} - \mathcal{P}_{\pm} \mathcal{P}'_{\pm} \right) \tilde{\mathcal{Z}}^{\pm}, \quad \tilde{\mathcal{Z}}^{\pm}(\lambda_0) = R_{\pm}(\lambda_0),$$

where $'$ denotes the differentiation with respect to λ . This prescription is also minimal in the sense that $\mathcal{P}_{\pm} R'_{\pm} = 0$.

We now continue the construction of the approximate Evans function. As a consequence of (6.10), for large L we set:

$$\begin{aligned} \mathcal{Z}^+(L, \lambda) &\sim \mathcal{Z}_{app}^+(L, \lambda) := e^{\text{tr}(\mathcal{A}_+(\lambda)|_{\mathcal{S}(\lambda)})L} \tilde{\mathcal{Z}}_1^+(\lambda) \wedge \dots \wedge \tilde{\mathcal{Z}}_k^+(\lambda), \\ \mathcal{Z}^-(-L, \lambda) &\sim \mathcal{Z}_{app}^-(-L, \lambda) := e^{-\text{tr}(\mathcal{A}_-(\lambda)|_{\mathcal{U}(\lambda)})L} \tilde{\mathcal{Z}}_{k+1}^-(\lambda) \wedge \dots \wedge \tilde{\mathcal{Z}}_N^-(\lambda). \end{aligned}$$

The objective is now to trace the evolution of the differential form $\mathcal{Z}_{app}^+(\cdot, \lambda)$ backward in z , and the evolution of $\mathcal{Z}_{app}^-(\cdot, \lambda)$ forward in z , starting from, respectively, the initial data $\mathcal{Z}_{app}^+(L, \lambda)$ and $\mathcal{Z}_{app}^-(-L, \lambda)$, and according to the system as in (4.2):

$$(6.11) \quad \mathcal{Z}'_{app}(z, \lambda) = \mathcal{A}(z, \lambda) \mathcal{Z}_{app}(z, \lambda).$$

The numerical approximation of $D(\lambda)$ in (6.9) is then recovered through:

$$(6.12) \quad D(\lambda) \sim D_{app}(\lambda) := \mathcal{Z}_{app}^+(0, \lambda) \wedge \mathcal{Z}_{app}^-(0, \lambda).$$

To solve (6.11) for \mathcal{Z}_{app}^{\pm} we use the polar-coordinate method described in [HuZ], which encodes \mathcal{Z}_{app}^{\pm} as product of a complex scalar r^{\pm} and the exterior product Ω^{\pm} of an orthonormal basis $\{\omega_i^+\}$ of \mathcal{S} or, respectively, an orthonormal basis $\{\omega_i^-\}$ of \mathcal{U} :

$$\mathcal{Z}_{app}^{\pm}(z, \lambda) = r^{\pm}(z, \lambda) \Omega^{\pm}(z, \lambda), \quad \Omega^+ = \omega_1^+ \wedge \dots \wedge \omega_k^+, \quad \Omega^- = \omega_{k+1}^- \wedge \dots \wedge \omega_N^-.$$

The above quantities Ω evolve by some implementation (e.g. Drury’s method below) of continuous orthogonalization, where the “radius” r satisfies a scalar ODE slaved to Ω , related to Abel’s formula for evolution of a full Wronskian. Namely (6.11), is equivalent to:

$$(6.13) \quad \begin{aligned} \Omega'(z, \lambda) &= \left(\text{Id}_N - \Omega \Omega^* \right) \mathcal{A}(z, \lambda) \Omega(z, \lambda) \\ r'(z, \lambda) &= \text{tr} \left(\Omega^* \mathcal{A}(z, \lambda) \Omega \right) \cdot r(z, \lambda) \end{aligned}$$

and we recover, in view of (6.12):

$$D_{app}(\lambda) = r^+(0, \lambda) r^-(0, \lambda) \cdot \Omega^+(0, \lambda) \wedge \Omega^-(0, \lambda),$$

see [HuZ, Z2, Z3] for further details. The rationale for solving the system (6.13) for the decomposition of \mathcal{Z}_{app} , rather than the original (6.11) is that the imposition of orthonormality

on Ω prevents the collapse of the various columns (solutions) onto a single fastest-growing mode, as would otherwise be the case. For a discussion of this and other numerical issues connected with the polar coordinate method, see [HuZ, Z3].

The calculations of (6.13) for individual λ are carried out using MATLAB's `ode45` routine, an adaptive 4th-order Runge-Kutta-Fehlberg method (RKF45) with excellent accuracy and automatic error control. Typical runs involved roughly 60 mesh points per side, with error tolerance set to `AbsTol = 1e-8` and `RelTol = 1e-6`. To produce analytically varying Evans function output, the initializing bases $\{\tilde{Z}_i^\pm\}$ are chosen analytically using Kato's ODE [GZ, HuZ, BrZ, BHZ]. Numerical integration of Kato's ODE is carried out using a second-order algorithm introduced in [Z2, Z3].

6.3 Winding number computation

Recall that the Evans condition amounts to checking for the existence of unstable zeros of the integrated Evans function \tilde{D} , described in section 4.4. We first observe (Proposition 6.10 [HLZ]), that for shock profiles of the hyperbolic-parabolic systems of the type we consider, there holds:

$$(6.14) \quad \lim_{|\lambda| \rightarrow \infty} \frac{\tilde{D}(\lambda)}{e^{\alpha\sqrt{\lambda}}} = C \quad \text{uniformly on } Re \lambda \geq 0,$$

with constants α and $C \neq 0$. When \tilde{D} is initialized in the standard way on the real axis, so that $\tilde{D}(\lambda) = \tilde{D}(\bar{\lambda})$, α and C are necessarily real. The knowledge that limit in (6.14) exists allows actually to determine α and C by curve fitting of $\log \tilde{D}(\lambda) = \log C + \alpha\lambda^{1/2}$ with respect to $\lambda^{1/2}$, for large $|\lambda|$.

One further determines the radius $R > 0$ so that:

$$\tilde{D}(\lambda) \neq 0 \quad \text{for } |\lambda| \geq R \text{ and } Re \lambda \geq 0,$$

by taking R to be a value for which the relative error between $\tilde{D}(\lambda)$ and $Ce^{\alpha\sqrt{\lambda}}$ becomes less than 0.2 on the entire semicircle:

$$S_R = \partial \left(B(0, R) \cap \{Re \lambda \geq 0\} \right),$$

indicating sufficient convergence to ensure nonvanishing. For many parameter combinations, $R = 2$ was sufficiently large. Alternatively, we could use energy estimates or direct tracking bounds as in [HLZ] and [HLyZ], respectively, to eliminate the possibility of eigenvalues of sufficiently high frequency. However, we have found the convergence study to be much more efficient in practice; see [HLyZ].

We now compute the winding number $I(R)$ of the image curve $\tilde{D}(S_R)$ with respect to 0, which equals the degree of the 2d vector field given by \tilde{D} in the interior region of S_R . Since the index of any nondegenerate zero of a holomorphic function is +1, the condition

$$I(R) = 0$$

is hence equivalent to \tilde{D} having no zeros in the open interior of the curve S_R . Since all the shocks considered here are of Lax or overcompressive type, condition $I(R) = 0$ is equivalent to the Evans stability condition (\tilde{D}).

The winding number $I(R)$ is now computed by varying values of λ along 20 points of the contour S , with mesh size taken quadratic in modulus to concentrate sample points near the origin where angles change more quickly, and summing the resulting changes in $\arg(\tilde{D}(\lambda))$, using $\Im \log \tilde{D}(\lambda) = \arg \tilde{D}(\lambda) \pmod{2\pi}$. To ensure winding number accuracy, we test a posteriori that the change in \tilde{D} for each step is less than 0.2, and add mesh points as necessary to achieve this. (Recall, by Rouché’s Theorem, that accuracy is preserved so long as relative variation of \tilde{D} along each mesh interval is ≤ 1.0 .) In Tables 2 and 1 we give the radius of the domain contour, the number of mesh points, the relative error for change in argument of $\tilde{D}(\lambda)$ between steps, and the numerical approximation of spatial infinity $\pm L$.

6.4 Results of numerical experiments

In our numerical study, we sampled from a broad range of parameters and checked stability of the resulting Lax and over-compressive profiles whenever their endstates fell into the hyperbolic region as required by our stability framework. We did not find any undercompressive profiles for the model considered here, either in the incompressible shear or the compressible case, nor did Antman and Malek–Madani find undercompressive profiles in

α	s	R	points	error	L	α	s	R	points	error	L
0.2	1.8	2	38	0.1947	16.25	1	1.8	2	27	0.1787	6.3
1	2.8	2	21	0.1791	2.5	2	2.8	2	21	0.1878	3
3	3.8	2	20	0.1103	1.8	5	5.8	2	20	0.0903	1.05

Table 1: Table demonstrating contour radius, number of mesh points, relative error, and spatial domain for the incompressible case.

α_2	α_3	s	R	points	error	L	α_2	α_3	s	R	points	rel error	L
0.1	1	1.9	2	20	0.13	15.01	0.1	6.6	9.5	2	20	0.00	2.01
0.9	2.6	8.7	2	20	0.01	2.01	1.3	3.4	8.3	2	20	0.01	2.01
3.7	4.2	7.1	2	20	0.02	2.01	1.7	0.2	3.9	2	20	0.08	19.01
6.1	2.6	8.7	2	20	0.01	2.01	4.1	4.6	8.3	2	20	0.01	2.01
6.9	0.6	8.3	4	20	0.17	7.01	6.9	0.2	8.3	2	20	0.12	15.01

Table 2: Table demonstrating contour radius, number of mesh points, relative error, and spatial domain. The data on the left side corresponds to the compressible 2D system, and that on the right to the transverse system.

their investigations of the incompressible shear case [AM]. As shown in Section D, undercompressive connections cannot occur in the incompressible shear case for any choice of potential. However, we do not see why they could not occur for other choices of elastic potential in the compressible case.

All our computations yielded zero winding number, consistent with stability. All together, our study consisted of over 8,000 Evans function computations. The following parameter combinations were examined for Evans stability.

The 2D incompressible shear case. The following parameter combinations yielded Evans function output with winding number zero, consistent with stability:

$$(\alpha, s) \in \{0.2 : 0.2 : 5\} \times \{0.2 : 0.2 : 7\}.$$

The 2D compressible case. In the compressible 2D case and the transverse case following, we computed the Evans function for the stated parameter combinations whenever the profile end-states did not lie in the elliptic region. For $\alpha_2 \neq 0$, we restricted our attention to the profiles connecting rest-points corresponding to solutions of (5.16) in the interval $[-50, 50]$.

We computed the Evans function for all 2 point configurations (Lax connections) coming from the following parameter combinations. All computations yielded zero winding number, consistent with stability:

$$\begin{aligned} (\alpha_2, \alpha_3, s) &\in \{0\} \times \{1.1 : 0.5 : 25.6\} \times \{0.5 : 0.5 : 20\}, \\ (\alpha_2, \alpha_3, s) &\in \{0.1 : 0.4 : 25.3\} \times \{0.2 : 0.4 : 25.4\} \times \{0.3 : 0.4 : 25.5\}. \end{aligned}$$

For the following parameter combinations, we investigated the 4 point configurations computing all Lax connections, and 5 overcompressive connections passing through evenly spaced points on the segment in phase space connecting the saddle points:

$$\begin{aligned} (\alpha_2, \alpha_3, s) &\in \{0\} \times \{0.03 : 0.07 : 1.03\} \times \{0.05 : 0.07 : 1.05\}, \\ (\alpha_2, \alpha_3, s) &= \{(0.08, 0.59, 0.75), (0.08, 0.87, 0.82), (0.22, 0.66, 0.75)\}. \end{aligned}$$

The transverse case. We computed the transverse Evans function for the two point configurations (Lax connections) for the following parameter combinations:

$$(\alpha_2, \alpha_3, s) \in \{0.1 : 0.4 : 25.3\} \times \{0.2 : 0.4 : 25.4\} \times \{0.3 : 0.4 : 25.5\}.$$

In addition we examined the 4 point configuration corresponding to $(\alpha_2, \alpha_3, s) = (0.1, 0.8, 0.8)$ computing the Evans function for the 4 Lax connections and for 5 overcompressive connections passing through points evenly spaced along the line in phase space between the two saddle points.

6.4.1 Numerical performance

The Evans function computations for the most part worked reliably and well, showing performance comparable to that seen in previous studies for gas dynamics [HLZ, HLyZ]

and MHD [BHZ, BLZ]. A typical winding number computation for a single profile took approximately 30 seconds and computation of the profile approximately 5 seconds.

As expected, performance degraded catastrophically in various boundary situations: the small-amplitude limit as $\frac{|a_+ - a_-|}{|a_+| + |a_-|} \rightarrow 0$; the characteristic limit as one or more characteristic speeds approach the shock speed; the large-amplitude limit as $|a_{\pm}|$ approach infinity or a_3 approaches the physical (infinite compression) boundary $a_3 = 0$; and the elliptic limit as one or both endstates a_{\pm} approach the elliptic region where characteristic speeds are complex. For discussion of causes of and (partial) cures for these numerical issues, see, e.g., [HLZ, BHZ, BLZ, Z3]. In the present study, such boundary cases were omitted.

7 Discussion and open problems

In this paper, we have obtained the first analytical stability results for viscoelastic shock waves, stability of small-amplitude Lax shocks, and set up a theoretical framework for future numerical and analytical studies of shock waves of essentially arbitrary viscoelastic models. A large-scale numerical Evans study for the canonical model (2.7) yielded a result of numerical stability for each of the more than 8,000 profiles tested, of both classical Lax and nonclassical overcompressive type, and with amplitudes varying from near zero to 50.

Interesting problems for the future are the treatment of more realistic potentials with physically correct asymptotic behavior, systematic numerical and asymptotic investigation across parameters as in [HLZ, HLYZ, BHZ, BLZ], and the treatment of phase transitional elasticity by incorporation of dispersive surface energy terms.

A Appendix: General facts

Though the investigations of this paper were carried out for special choices of W , \mathcal{Z} , the methods we use apply to much more general choices. With an eye toward future work, we collect in this appendix the information needed to carry out such extensions.

A.1 General elastic potential

Theorem A.1. *Let $W : \mathbb{R}^{3 \times 3} \rightarrow \overline{\mathbb{R}}_+$ satisfy (2.4) and (2.6). Then there exists a scalar function $\sigma : \mathbb{R}^3 \rightarrow \overline{\mathbb{R}}_+$, such that:*

$$W(F) = \sigma(|F|^2, |FF^T|^2, \det F).$$

The derivative $DW(F) \in \mathbb{R}^{3 \times 3}$, wherever defined at $F \in \mathbb{R}^{3 \times 3}$ (so that $\partial_A W(F) = DW(F) : A$), is given by:

$$DW(F) = \nabla \sigma(|F|^2, |FF^T|^2, \det F) \cdot \left(2F, 4FF^T F, \text{cof } F \right).$$

If $W(\text{Id}) = 0$ and W is \mathcal{C}^2 in a neighborhood of $SO(3)$, then:

$$DW(\text{Id}) = 0, \quad D^2W(\text{Id}) : A = \lambda(\text{tr} A)\text{Id} + \mu \text{sym} A \quad \forall A \in \mathbb{R}^{3 \times 3},$$

with the convention $\partial_{A_1, A}^2 W(\text{Id}) = (D^2 W(\text{Id}) : A) : A_1$ and the Lamé constants λ and μ :

$$\lambda = \nabla^2 \sigma(3, 3, 1) : \left((2, 4, 1) \otimes (2, 4, 1) \right), \quad \mu = \nabla \sigma(3, 3, 1) \cdot (0, 8, -2)$$

satisfying: $\mu \geq 0$ and $3\lambda + \mu \geq 0$.

Proof. According to the representation theorem [TN], every frame invariant and isotropic W depends only on the principal invariants of the left Cauchy deformation tensor FF^T , that is $W(F) = \bar{\sigma}(\text{tr}(FF^T), \text{tr} \text{ cof}(FF^T), \det(FF^T))$. Since $\text{tr} \text{ cof} Q = \frac{1}{2}(\text{tr} Q)^2 - \frac{1}{2}\text{tr}(Q^2)$, the claim on the form of W follows directly.

The formula for derivative $DW(F)$ follows from:

$$\partial_A |F|^2 = 2F : A, \quad \partial_A |FF^T|^2 = 4FF^T F : A, \quad \partial_A \det F = \text{cof} F : A,$$

where for the last expression we used $\det(F + Q) = \det F + F : \text{cof} Q + Q : \text{cof} F + \det Q$, valid for 3×3 matrices F, Q .

The vanishing of $DW(\text{Id})$ is clear since W is minimized at Id . The formula for $D^2 W(\text{Id})$ follows by chain rule and Lemma A.2. Further, notice that $\partial^2 W_{A, A}(\text{Id}) \geq 0$, which reads:

$$(A.1) \quad \lambda |\text{tr} A|^2 + \mu |\text{sym} A|^2 \geq 0 \quad \forall A \in \mathbb{R}^{3 \times 3}.$$

Evaluating (A.1) first at a traceless A and then at $A = \text{Id}$ we see that:

$$(A.2) \quad \mu \geq 0, \quad 3\lambda + \mu \geq 0.$$

To prove that (A.2) implies (A.1), write $\text{sym} A$ as the sum of orthogonal matrices: $\text{sym} A = \text{diag}(a_{11}, a_{22}, a_{33}) + B$. Then: $|\text{sym} A|^2 = \sum_{i=1}^3 a_{ii}^2 + |B|^2$, so:

$$\lambda |\text{tr} A|^2 + \mu |\text{sym} A|^2 = \lambda \left(\sum_{i=1}^3 a_{ii} \right)^2 + \mu \sum_{i=1}^3 a_{ii}^2 + \mu |B|^2 \geq (\lambda + \mu/3) \left(\sum_{i=1}^3 a_{ii} \right)^2 + \mu |B|^2,$$

which ends the proof. ■

For the behavior of W close to the energy well $SO(3)$ it is important to know the derivatives of W at $R \in SO(3)$. It follows by frame invariance that:

$$\partial_{RF_1, \dots, RF_n}^n W(R) = \partial_{F_1, \dots, F_n}^n W(\text{Id}) \quad \forall F_1 \dots F_n \in \mathbb{R}^{3 \times 3} \quad \forall R \in SO(3).$$

Hence, it suffices to find the derivatives of W at Id . Direct calculation yields the following:

Lemma A.2. *For $F \in \mathbb{R}^{3 \times 3}$, let $\alpha(F) = |F|^2$, $\beta(F) = |FF^T|^2$ and $\gamma(F) = \det F$. Then, for any $A_1, A \in \mathbb{R}^{3 \times 3}$ we have:*

$$\begin{aligned} (\alpha, \beta, \gamma)(\text{Id}) &= (3, 3, 1) \\ \partial_{A_1}(\alpha, \beta, \gamma)(\text{Id}) &= \left(\text{Id} : A_1 \right) (2, 4, 1) \\ \partial_{A_1, A}^2(\alpha, \beta, \gamma)(\text{Id}) &= \left(A : A_1 \right) (2, 4, 1) + \left(\text{sym} A : A_1 \right) (0, 8, -2) \\ \partial_{A_1, A, A}^3(\alpha, \beta, \gamma)(\text{Id}) &= - \left(\text{cof} A : A_1 \right) (0, 8, -2) + \left((\text{cof} A + AA^T + 2A^2) : A_1 \right) (0, 8, 0) \\ \partial_{A_1, A, A, A}^4(\alpha, \beta, \gamma)(\text{Id}) &= 3 \left((AA^T A) : A_1 \right) (0, 8, 0) \end{aligned}$$

For F as in (3.1), we have:

$$\alpha(F) = 2 + |a|^2, \quad \beta(F) = 2 + |a|^4 + 2(|a|^2 - a_3^2), \quad \gamma(F) = a_3.$$

Hence, and without loss of generality, the reduced function $W(a)$ must be of the form $W(a) = \tilde{\sigma}(|a|^2, a_3)$, for some $\tilde{\sigma} : \mathbb{R}^2 \rightarrow \bar{\mathbb{R}}_+$.

In the incompressible shear case, it reduces to:

$$(A.3) \quad \check{W}(a) = \check{\sigma}(|a|^2) = \tilde{\sigma}(|a|^2, 1),$$

leading to a profile equation agreeing with that of the 2×2 rotationally symmetric model:

$$(A.4) \quad a_t + (2\nabla\check{\sigma}(|a|^2)a)_z = a_{zz}.$$

This clarifies and puts in a more familiar context the investigations of Antman and Malek-Madani [AM] on existence of viscous profiles for the 2D incompressible shear model.

A.2 General viscous stress tensor

We do not have a complete categorization of possible \mathcal{Z} satisfying (i)–(iii) corresponding to that of Theorem A.1 for the elastic energy density W . However, we note the related discussion of Antman [A] for the class of systems of *strain-rate type*:

$$\mathcal{Z}(F, Q) = FS(C, D),$$

where S is a symmetric dissipation tensor depending on the the metric $C = F^T F$ and on its time derivative $D = F^T Q + Q^T F = 2\text{sym}(F^T Q)$. These automatically satisfy (i) and (ii) because $\text{sym}((RF)^T(RKF + RQ)) = \text{sym}(F^T Q + F^T KF) = \text{sym}(F^T Q)$. Thus only (iii) need be checked, in the form:

$$(A.5) \quad S(C, D) : D \geq 0.$$

Both of the examples (2.9) are of this type. For $\mathcal{Z}_1 = FS_1$, we have:

$$S_1(C, D) = \text{sym}(F^T Q) = \frac{1}{2}D,$$

which evidently satisfies the strict version of inequality (A.5):

$$(A.6) \quad S(C, D) : D \geq \gamma|D|^2, \quad \gamma > 0.$$

For $\mathcal{Z}_2 = FS_2$, we have $S_2 = (\det F)F^{-1}\text{sym}(QF^{-1})F^{-1,T} = \frac{1}{2}(\det C)^{1/2}C^{-1}DC^{-1}$, hence:

$$S_2(C, D) : D = \frac{1}{2}(\det C)^{1/2}C^{-1}C_t C^{-1} : D = \frac{1}{2}(\det C)^{1/2}|C^{-1/2}DC^{-1/2}|^2 \geq \gamma|D|^2,$$

where γ depends on C , but is uniform for F bounded and $\det F$ bounded away from zero.

In [A], Antman proposes as a sufficient condition for (A.6), that S be monotone in D in the sense that $\frac{\partial S}{\partial D}A : A \geq \gamma|A|^2$, $\gamma > 0$, for A symmetric. This implies (A.6) under the additional assumption $S(\cdot, 0) \equiv 0$ (i.e. viscous force vanishes at zero velocity), by:

$$S(C, D) : D - S(C, 0) : D = \int_0^1 \frac{\partial S}{\partial D}(C, \theta D)D : D \, d\theta \geq \gamma|D|^2.$$

It is easily checked that monotonicity holds for both of the choices $\mathcal{Z}_1, \mathcal{Z}_2$.

B Appendix: Phase-transitional elasticity

Another interesting direction for future investigations is the phase-transitional case, as we now briefly discuss. A typical model, as described in [FP], has the form:

$$W(F) = |F^T F - C_-|^2 \cdot |F^T F - C_+|^2,$$

where:

$$C_{\pm} = F_{\pm}^T F_{\pm} = \begin{bmatrix} 1 & 0 & 0 \\ 0 & 1 & \pm\varepsilon \\ 0 & \pm\varepsilon & 1 + \varepsilon^2 \end{bmatrix}, \quad F_{\pm} = \begin{bmatrix} 1 & 0 & 0 \\ 0 & 1 & \pm\varepsilon \\ 0 & 0 & 1 \end{bmatrix}.$$

Evidently, W is minimized among planar deformation gradients F at the two equilibria F_{\pm} .

A particularly interesting class of solutions to (2.1) are stationary phase-transitional shocks connecting the two equilibria (b_{\pm}, a_{\pm}) , $a_{\pm} = (0, \pm\varepsilon, 1)$, that is, zero-speed shocks compatible with the Rankine-Hugoniot condition for (3.11) with (3.3): $b_+ = b_-$, $DW(a_+) = DW(a_-)$. Similarly as in section 5 and as in 1d case treated by Slemrod [Sl], such connections do not exist under the viscoelastic effects alone, but their existence requires also the inclusion of third-order surface energy terms as in Section 2.3.

Solving the system (5.1) augmented by the term $\gamma \operatorname{div} \mathcal{E}$ coming from the surface energy \mathcal{E}_0 as in (2.11), we obtain (for $s = 0$) that $b = \text{const}$ and $DW(a)_z = \gamma a_{zzz}$. Take the capillarity coefficient $\gamma \neq 0$ and assume that $DW(a_{\pm}) = 0$ (the end-states in the potential well). Integrating, we obtain a harmonic oscillator equation: $DW(a) = \gamma a_{zz}$, with Hamiltonian:

$$H(a, a_z) = W(a) - \frac{\gamma}{2} |a_z|^2 = \text{const}.$$

Hence, a question is whether the connected component of the level set of H , containing $(a_-, 0)$, contains also $(a_+, 0)$. Contrary to the 1d case in [Sl], this is only a necessary condition for profile's existence. Existence or nonexistence of such connections would be an interesting question for further analytical and numerical investigation.

A second question would be to determine stability of such stationary transitions, should they exist. We conjecture that, similarly as in [Z8] for the 1d case, the spectral stability follows automatically by energy-considerations. Stability of nonstationary phase-transitional profiles has not been treated even in the 1d case, and would be another interesting problem.

Finally, we point out that the equations with surface energy do not fit the stability theory of Section 4, since they are third- and not second-order. However, we expect that the basic methods should still apply, after suitable modifications. It would be very interesting, for the sake of this and other applications involving dispersive phenomena (for example, the Hall effect in MHD), to carry out a complete analysis extending the nonlinear stability framework to this higher-order case.

C Appendix: Nonhyperbolic endstates

Consider the 1D compressible equations (3.20) with the associated profile equation, obtained by setting $a_1 = a_2 = 0$ in (5.8):

$$(C.1) \quad 2a_3' = (a_3^3 - a_3 - \sigma a_3) - (\alpha^3 - \alpha - \sigma\alpha), \quad \alpha := a_{3-} = a_3(-\infty).$$

As noticed in section 3.3.4, strict hyperbolicity of (3.20) corresponds to $|a_3| > 1/\sqrt{3}$. On the other hand, when $\alpha > a_{3+} > 0$, $\sqrt{(1+\sigma)/3} < \alpha < \sqrt{1+\sigma}$ and $\sigma = a_{3+}^2 + a_{3+}\alpha + \alpha^2 > 0$, the equation (C.1) possesses a solution $a_3(z)$, decreasing from its unstable equilibrium $\alpha = a_3(-\infty)$ to the stable one $a_{3+} = a_3(+\infty)$. This solution corresponds to a viscous shock profile of the associated scalar equation $a_{3,t} + (a_3^3 - a_3)_z = a_{3,zz}$ and the 2d viscous system:

$$(C.2) \quad a_{3,t} - b_{3,z} = 0, \quad b_{3,t} - (a_3^2 - a_3)_z = b_{3,zz}.$$

Thus, there exist shock profiles of (3.20) for which the left end-state is hyperbolic, with one characteristic greater than the shock speed s and the other smaller than s , but the right end-state is not hyperbolic as it has two pure imaginary characteristics with real parts $c_+ < s$. This is a “complex Lax shock” of the type considered in [AMPZ, OZ].

Writing the system (C.2) in the operator form $(a_3, b_3)_t^T = Q \cdot (a_3, b_3)^T$ where:

$$Q = \begin{bmatrix} 0 & \partial_z \\ (3a_3^2 - 1)\partial_z & \partial_{zz} \end{bmatrix},$$

we determine the spectrum of the constant solution (a_+, b_+) through the dispersion relation:

$$0 = \det \begin{bmatrix} \lambda & -ik \\ -(3a_{3+}^2 - 1)ik & \lambda + k^2 \end{bmatrix} = \lambda^2 + k^2\lambda + (3a_{3+}^2 - 1)k^2.$$

Consequently:

$$\lambda(k) \sim -\frac{1}{2}k^2 \pm k\sqrt{1 - 3a_{3+}^2} \quad \text{for } k \sim 0,$$

yielding a maximal growth rate e^{rt} with $r = \text{Re } \lambda_{\max}(k) \sim (1 - 3a_{3+}^2)/2$. As discussed in [AMPZ, OZ], for speed $|s|$ sufficiently large compared to the growth rate r , the shock profile can be seen to be stable, despite instability of its right end-state as a constant solution. It also can be shown, by weighted coordinate techniques as in [Sat, LRTZ], that Evans stability together with such a convection vs. growth condition on the essential spectrum, implies linearized and nonlinear stability for perturbations that are exponentially localized on the half-line $z > 0$. Another direction for further investigation might be to understand whether there are interesting physical phenomena corresponding to shocks of this type.

In contrast with the situations considered in [AMPZ, OZ], for which profiles associated with complex Lax shocks are oscillatory at the complex end, the profiles here are of ordinary monotone type. Other complex Lax connections, genuinely two-dimensional, may be seen in Fig. 2(b). Provided that all characteristics are incoming on the complex side $z \rightarrow +\infty$, nonlinear stability may again be established by weighted norm methods assuming Evans stability plus an appropriate convection vs. growth condition as described in [AMPZ, OZ].

D Appendix: Nonexistence of undercompressive profiles

We show that undercompressive profiles do not occur for general shear models as in (A.3). The same argument implies that undercompressive profiles cannot occur also in the 2D compressible case, for the special class of potentials $W(a)$ depending only on $|a|^2$.

Note first that every undercompressive profile $(a(z), b(z))$ of (3.15), with speed s , induces an undercompressive profile of (5.9) given by $z \mapsto a(sz)$ with speed $\sigma = s^2$. This statement follows from a more general observation in [MaZ3, BLZ] relating the type of inviscid shocks to the connection number for the traveling wave in the reduced ODE (5.2). Alternatively, the same can be checked directly: if the sum of the number of eigenvalues λ for (3.15) at $a(-\infty)$ with $\lambda > s$, and the number of eigenvalues μ at $a(+\infty)$ with $\mu < s$, is less than 5 (the dimension of the system increased by 1), then the sum of the number of eigenvalues of (5.9) $\lambda^2 > \sigma$ and the number of eigenvalues $\mu^2 < \sigma$ is less than 3, when $s > 0$. When $s < 0$ we likewise have that the number of $\mu^2 < \sigma$ plus the number of $\mu^2 > \sigma$, is less than 3.

We shall prove that the system:

$$(D.1) \quad a_t + (h(|a|^2)a)_z = a_{zz},$$

generalizing (5.9) and (A.4), where $h = 2\nabla\sigma$, admits no undercompressive shocks.

After integrating in z , the traveling wave ODE for (D.1) reads:

$$(D.2) \quad a' = -\sigma a + h(|a|^2)a - (-\sigma a_- + h(|a_-|^2)a_-),$$

where σ is the speed of the shock and $a_- = (a_{1-}, a_{2-}) = a(-\infty)$ is its left end-state. Note that all possible right end-states $a_+ = (a_{1+}, a_{2+})$ which can be connected to a_- , satisfying hence the Rankine-Hugoniot condition:

$$(D.3) \quad h(|a_-|^2)a_- - \sigma a_- = h(|a_+|^2)a_+ - \sigma a_+,$$

must lie on the same line through the origin, due to rotational invariance of the system (D.1). We may, without loss of generality, assume it to be the a_1 axis, so that: $a_{2-} = a_{2+} = 0$.

The gradient of the right hand side in (D.2):

$$D(h(|a|^2)a - \sigma a) = (h(|a|^2) - \sigma)\text{Id} + 2\nabla h(|a|^2)a \otimes a$$

has two eigenvalues: $\lambda_1(a) = h(|a|^2) - \sigma + 2\nabla h(|a|^2)|a|^2$, with the radial direction eigenvector a , and $\lambda_2(a) = h(|a|^2) - \sigma$ with the eigenvector a^\perp in the transverse (rotational) direction.

Observe further that an undercompressive shock profile must necessarily be a saddle to saddle connection, and that any saddle point has one of its invariant manifolds (the one corresponding to λ_1) confined to the a_1 axis. We find that the profile must either lie entirely on the a_1 axis, or else entirely off the axis, leaving a_- and entering a_+ along the transverse direction (orthogonal to the axis). We now distinguish 3 cases:

Case (i) $\mathbf{a}_{1+}\mathbf{a}_{1-} > \mathbf{0}$. In this situation, in view of (D.3), the transverse eigenvalues $\lambda_2(a_-) = h(a_{1-}^2) - \sigma$ and $\lambda_2(a_+) = h(a_{1+}^2) - \sigma$ must also have a common sign. Thus

the profiles may only leave or only enter along the transverse directions, contradicting the assumed behavior.

Case (ii) $\mathbf{a}_{1+}\mathbf{a}_{1-} < 0$, and the profile connection is radial. Without loss of generality, assume that $a_{1-} > 0$ and $a_{1+} > 0$ so that $a_1'(z) < 0$ along the whole profile. In particular, $a_1'(z_0) < 0$ at z_0 where $a_1(z_0) = 0$. By (D.2) it follows that:

$$h(a_{1-}^2)a_{1-} - \sigma a_{1-} = -a_1'(z_0) > 0,$$

hence $h(a_{1-}^2) - \sigma > 0$. This means that the transverse eigenvalue corresponds to the unstable direction, contradicting the profile being radial and a_- being a saddle equilibrium point.

Case (iii) $\mathbf{a}_{1+}\mathbf{a}_{1-} < 0$, and the profile connection is transverse. In this situation $\lambda_2(a_-) > 0$ and $\lambda_2(a_+) < 0$. Observe that on the circle $|a|^2 = a_{1-}^2$, we have:

$$a' = (h(a_{1-}^2) - \sigma)(a - a_-) = \lambda_2(a_-)(a - a_-),$$

and thus the exterior of this circle is a positively invariant set. Likewise, by (D.2) and (D.3), on the circle $|a|^2 = a_{1+}^2$ there holds:

$$a' = (h(a_{1+}^2) - \sigma)(a - a_+) = \lambda_2(a_+)(a - a_+),$$

and hence the exterior of this circle is a negatively invariant set. Consequently, at that of the two saddle points a_- and a_+ which has larger norm, the invariant curve tangent to the transverse direction must lie, for all times, outside the corresponding circle. This is clearly a contradiction and ends the proof, as the case $a_{1+} = -a_{1-}$ is ruled out by comparing the right hand sides of the above ODEs.

References

- [AGJ] J. Alexander, R. Gardner and C.K.R.T. Jones, *A topological invariant arising in the analysis of traveling waves*, J. Reine Angew. Math. 410 (1990) 167–212.
- [AS] J. C. Alexander and R. Sachs, *Linear instability of solitary waves of a Boussinesq-type equation: a computer assisted computation*, Nonlinear World, 2(4):471–507, 1995.
- [AMPZ] A. Azevedo, D. Marchesin, B. Plohr and K. Zumbrun, *Long-lasting diffusive solutions for systems of conservation laws*, VI Workshop on Partial Differential Equations, Part I (Rio de Janeiro, 1999). Mat. Contemp. 18 (2000), 1–29.
- [A] S. Antmann, *Real artificial viscosity for the equations of nonlinear elasticity*, draft (2010).
- [AM] S. Antmann and R. Malek-Madani, *Travelling waves in nonlinearly viscoelastic media and shock structure in elastic media*, Quart. Appl. Math. 46 (1988) 77–93.
- [Ba] J.M. Ball, *Some open problems in elasticity. Geometry, mechanics, and dynamics*, Springer, New York (2002), 3–59.
- [BHZ] B. Barker, J. Humpherys, and K. Zumbrun, *One-dimensional stability of parallel shock layers in isentropic magnetohydrodynamics*, preprint (2009).

- [BHRZ] B. Barker, J. Humpherys, , K. Rudd, and K. Zumbrun, *Stability of viscous shocks in isentropic gas dynamics*, Comm. Math. Phys. 281 (2008), no. 1, 231–249.
- [BDG] T.J. Bridges, G. Derks, and G. Gottwald, *Stability and instability of solitary waves of the fifth-order KdV equation: a numerical framework*. Phys. D 172 (2002), no. 1-4, 190–216.
- [BLZ] B. Barker, O. Lafitte, and K. Zumbrun, *Stability of 2d viscous isentropic MHD shocks with infinite electrical resistivity*, preprint (2009).
- [Be1] W.-J. Beyn, *The numerical computation of connecting orbits in dynamical systems*, IMA J. Numer. Analysis 9: 379–405 (1990).
- [Be2] W.-J. Beyn, *Zur stabilit at von differenzenverfahren für systeme linearer gewöhnlicher randwertaufgaben*, Numer. Math. 29: 209–226 (1978).
- [Br] L. Q. Brin, *Numerical testing of the stability of viscous shock waves*. Math. Comp. 70 (2001) 235, 1071–1088.
- [BrZ] L. Brin and K. Zumbrun, *Analytically varying eigenvectors and the stability of viscous shock waves*. Seventh Workshop on Partial Differential Equations, Part I (Rio de Janeiro, 2001). Mat. Contemp. 22 (2002), 19–32.
- [CGS] J. Carr, M. Gurtin, and M. Slemrod, *Structured phase transitions on a finite interval*, Arch. Rational Mech. Anal. (86) (1984), 317–351.
- [CS1] C. C. Conley and J.Smoller, *On the structure of magnetohydrodynamic shock waves*, Comm. Pure Appl. Math 27, 367–375, 1974.
- [CS2] C. C. Conley and J.Smoller, *On the structure of magnetohydrodynamic shock waves. II*, J. Math. Pures Appl. (9) no. 4, 429–443, 1975.
- [CHNZ] N. Costanzino, J. Humpherys, T. Nguyen, and K. Zumbrun, *Spectral stability of noncharacteristic boundary layers of isentropic Navier–Stokes equations*, to appear, Arch. Rat. Mechanics and Anal.
- [D] C. Dafermos, *Hyperbolic Conservation Laws in Continuum Physics*, Springer-Verlag 1999.
- [EF] J. W. Evans and J. A. Feroe. *Traveling waves of infinitely many pulses in nerve equations*, Math. Biosci., 37:23–50 (1977).
- [F] H. Freistühler, *Dynamical stability and vanishing viscosity: a case study of a non-strictly hyperbolic system*, Comm. Pure Appl. Math. 45 (1992).
- [FP] H. Freistühler and R. Plaza, *Normal modes and nonlinear stability behaviour of dynamic phase boundaries in elastic materials*, Arch. Ration. Mech. Anal. 186 (2007), no. 1, 1–24.
- [FS] H. Freistühler and P. Szmolyan, *Existence and bifurcation of viscous profiles for all intermediate magnetohydrodynamic shock waves*, SIAM J. Math. Anal. 26 no. 1 (1995) 112–128.
- [GJ1] R. Gardner and C.K.R.T. Jones, *A stability index for steady state solutions of boundary value problems for parabolic systems*, J. Diff. Eqs. 91, no. 2, 181–203, 1991.
- [GJ2] R. Gardner and C.K.R.T. Jones, *Traveling waves of a perturbed diffusion equation arising in a phase field model*, Ind. Univ. Math. J. 38, no. 4, 1197–1222, 1989.

- [GZ] R. Gardner and K. Zumbrun, *The Gap Lemma and geometric criteria for instability of viscous shock profiles*. Comm. Pure Appl. Math. 51 (1998), no. 7, 797–855.
- [G] P. Germain, *Contribution à la théorie des ondes de choc en magnétodynamique des fluides*, ONERA Publ. No. 97, Office Nat. ?tudes et Recherche A?rospatiales, Châtillon, 1959.
- [HM] N. Hale and D. R. Moore. *A sixth-order extension to the matlab package bvp4c of j. kierzenka and l. shampine*, Technical Report NA-08/04, Oxford University Computing Laboratory, May 2008.
- [HZ] P. Howard and K. Zumbrun, *Stability of undercompressive viscous shock waves*, J. Differential Equations 225 (2006), no. 1, 308–360; preprint 2004.
- [HR] P. Howard and M. Raoofi, *Pointwise asymptotic behavior of perturbed viscous shock profiles*, Adv. Differential Equations (2006) 1031–1080.
- [HRZ] P. Howard, M. Raoofi, and K. Zumbrun, *Sharp pointwise bounds for perturbed viscous shock waves*, J. Hyperbolic Differ. Equ. (2006) 297–373; preprint 2005.
- [HLZ] J. Humpherys, O. Lafitte, and K. Zumbrun, *Stability of viscous shock profiles in the high Mach number limit*, to appear, Comm. Math. Phys.; published online, Sept. 2009.
- [HLyZ] J. Humpherys, G. Lyng, and K. Zumbrun, *Spectral stability of ideal gas shock layers*, To appear, Arch. for Rat. Mech. Anal.
- [HuZ] J. Humpherys and K. Zumbrun, *Spectral stability of small amplitude shock profiles for dissipative symmetric hyperbolic–parabolic systems*. Z. Angew. Math. Phys. 53 (2002) 20–34.
- [HuZ2] J. Humpherys and K. Zumbrun, *An efficient shooting algorithm for Evans function calculations in large systems*, Phys. D 220 (2006), no. 2, 116–126.
- [K] T. Kato, *Perturbation theory for linear operators*, Springer-Verlag, Berlin Heidelberg (1885).
- [Kaw] S. Kawashima, *Systems of a hyperbolic–parabolic composite type, with applications to the equations of magnetohydrodynamics*, PhD thesis, Kyoto University (1983).
- [KL] J. Kierzenka and L. F. Shampine. *A BVP solver that controls residual and error*, JNAIAM J. Numer. Anal. Ind. Appl. Math., 3(1-2):27–41, 2008.
- [LZu] T.P. Liu and K. Zumbrun, *On nonlinear stability of general undercompressive viscous shock waves*, Commun. Math. Phys. 174 (1995) 319–345.
- [LRTZ] G. Lyng, M. Raoofi, B. Texier, and K. Zumbrun, *Pointwise Green function bounds and stability of combustion waves*, J. Differential Equations 233 (2007), no. 2, 654–698.
- [MaZ2] C. Mascia and K. Zumbrun, *Stability of small-amplitude shock profiles of symmetric hyperbolic-parabolic systems*, Comm. Pure Appl. Math. 57 (2004), no. 7, 841–876.
- [MaZ3] C. Mascia and K. Zumbrun, *Pointwise Green function bounds for shock profiles of systems with real viscosity*. Arch. Ration. Mech. Anal. 169 (2003), no. 3, 177–263;
- [MaZ4] C. Mascia and K. Zumbrun, *Stability of large-amplitude viscous shock profiles of hyperbolic-parabolic systems*, Arch. Ration. Mech. Anal. 172 (2004), no. 1, 93–131;
- [OZ] M. Oh and K. Zumbrun, *Stability of periodic solutions of viscous conservation laws with viscosity- 1. Analysis of the Evans function*, Arch. Ration. Mech. Anal. 166 (2003), no. 2, 99–166.

- [PSW] R. L. Pego, P. Smereka, and M. I. Weinstein. *Oscillatory instability of traveling waves for a KdV-Burgers equation*, Phys. D, 67(1-3):45–65, 1993.
- [R] M. Raoofi, *L^p asymptotic behavior of perturbed viscous shock profiles*, J. Hyperbolic Differ. Equ. 2 (2005), no. 3, 595–644; preprint 2004.
- [RZ] M. Raoofi and K. Zumbrun, *Stability of undercompressive viscous shock profiles of hyperbolic-parabolic systems*, J. Differential Equations, (2009) 1539–1567.
- [Sat] D. Sattinger, *On the stability of waves of nonlinear parabolic systems*. Adv. Math. 22 (1976) 312–355.
- [SGT] L. F. Shampine, I. Gladwell, and S. Thompson. *Solving ODEs with MATLAB*. Cambridge University Press, Cambridge (2003).
- [Sl] M. Slemrod, *Dynamics of first-order phase transitions*, in: Phase transitions and material instabilities in solids, ed. M.E. Gurtin, Academic Press (1984) 163–203.
- [SZ] P. Sternberg and K. Zumbrun, *Connectivity of Phase Boundaries in Strictly Convex Domains*, Arch. Rational:Mech. Anal. 141 (1998), no. 4, 375–400.
- [TN] C. Truesdell and W. Noll, *The non-linear field theories of mechanics*, Third edition. Edited and with a preface by Stuart S. Antman. Springer-Verlag, Berlin, 2004. xxx+602 pp. ISBN: 3-540-02779-3.
- [Z2] K. Zumbrun. *A local greedy algorithm and higher order extensions for global numerical continuation of analytically varying subspaces*, to appear, Quart. Appl. Math.
- [Z3] K. Zumbrun. *Numerical error analysis for evans function computations: a numerical gap lemma, centered-coordinate methods, and the unreasonable effectiveness of continuous orthogonalization*, preprint, 2009.
- [Z4] K. Zumbrun, *Stability of large-amplitude shock waves of compressible Navier–Stokes equations*, with an appendix by Helge Kristian Jenssen and Gregory Lyng, in Handbook of mathematical fluid dynamics. Vol. III, 311–533, North-Holland, Amsterdam, (2004).
- [Z8] K. Zumbrun, *Dynamical stability of phase transitions in the p -system with viscosity-capillarity*, SIAM J. Appl. Math. 60 (2000), no. 6, 1913–1924 (electronic).
- [ZH] K. Zumbrun and P. Howard, *Pointwise semigroup methods and stability of viscous shock waves*. Indiana Mathematics Journal V47 (1998), 741–871; Errata, Indiana Univ. Math. J. 51 (2002), no. 4, 1017–1021.